The Pennsylvania State University

The Graduate School

MATERIAL EXTRUSION ADDITIVE MANUFACTURING OF THERMOSET AND THERMOPLASTIC COMPOSITES

A Thesis in

Additive Manufacturing and Design

by

Lachlan M. Peeke

Submitted in Partial Fulfillment
of the Requirements
for the Degree of

Master of Science

August 2021

The thesis of Lachlan M. Peeke was reviewed and approved by the following:

Michael Hickner

Professor of Materials Science and Engineering, Chemical Engineering, and Chemistry

Thesis Adviser

Nicholas Meisel

Assistant Professor of Engineering Design

Timothy Simpson

Professor of Engineering Design and Manufacturing

Head of the Department of Additive Manufacturing and Design

ABSTRACT

Additive manufacturing (AM) is a disruptive new manufacturing process that gives designers freedom for creating highly complex shapes through free-form fabrication. Through the layer-by-layer process, engineers have been able to mix and match different materials inside one geometry to create novel composites. One of the downsides of the current technology is the limited number of materials available for AM. The majority of polymers used in extrusion AM are thermoplastics because they are easy to process in affordable machines. While mechanically robust, thermoplastics are known to weaken with increases in temperature or exposure to solvents. Traditional manufacturing has a much larger variety of polymers available with a wide array of unique properties such as chemical resistance or biocompatibility. These unique properties can be achieved through different types of thermosetting polymers such as silicone. Silicone-based products can be found everywhere from medical devices to engine seals. With AM, a composite structure of thermoplastics and thermosets would yield an end product with mechanical strength and chemical properties that exceed the individual materials.

This work consists of three main sections: (1) the processes developed to support the printing of the dual material composites, (2) tensile tests to demonstrate the result of thermoplastic reinforcement patterns in a silicone matrix, and (3) a study on the shear-thinning trends of silicones to describe ideal flow properties. The key innovation of this work is a new process that was developed to print reinforced silicone components. This process relied on a multi-material approach to place silicone and reinforcement in any desired location in the printed part. Although much research touches on the multi-material aspect of AM, the process presented manipulates two dissimilar materials in one system. Individually, thermoplastics and thermosets have been printed with similar thermoplastic and thermoset materials. The process hinges on the combination of a fused filament thermoplastic extruder and a pneumatic fluidic dispenser, both of which are mounted on a 3-axis gantry and controlled through software-generated machine code. Tensile data was collected by printing three-layer composite structures out of high viscosity silicone and patterned meshes of commonly used thermoplastics in AM. To complement the new process developed in this work for fabricating multi-material reinforced silicones, flow properties of various silicone feedstocks were identified through collection and observation of material

throughput out of the fluidic dispenser under various pressure inputs to the system. By developing a dual extrusion 3D printer that can process common thermoplastics with commercially available thermosetting silicones, the end product can demonstrate the best mechanical and chemical properties of each material. This work sets the stage for generalizable direct ink writing and fused filament fabrication of architected elastomers where hard and soft components can be designed into the three-dimensional structure of the part.

TABLE OF CONTENTS

List of Tables

List of Figures

Acknowledgments

I would like to thank my advisor, Mike Hickner, for pushing me to strive for excellence as a student and a researcher. With his guidance and support, I come away from this Master’s program a new with a wealth of knowledge both as an academic and professional.

I would also like to acknowledge the Penn State 3D Printing Club (2014-2021). Thanks to these wonderful people, I started my journey into the world of 3D printing. Their unbridled passion for creating and connecting with others is still something I plan to carry forward into the next adventure.

Lastly, I would like to thank the never-ending support of my family. This Master’s program was a journey and I am glad they had my back through it all.

Chapter 1

Introduction

This chapter provides the background, motivations, objectives, and scope of the work. The background reviews the current types of additive manufacturing machines, discusses the materials commonly used, and identifies the current limitations of this technology. This chapter highlights the importance of the development of the dual material thermoplastic and thermoset 3D printer that can reliably print composite structures. The main objective and scope of this work are to develop and optimize this dual material 3D printer, print and characterize composite structures, and evaluate a series of commercially available silicones to define selection criteria for further work. The organization of the report gives an overview of the content of this thesis.

1.1 Background

Additive manufacturing (AM) is currently a disruptive technology that is breaking new ground in the manufacturing market. Using the layer-by-layer approach, AM gives designers nearly limitless complexity and removes significant design constraints common in traditional subtractive manufacturing. Many AM processes currently use thermoplastics or metal powders. These materials are often used in injection molding. Newer AM processes use unique materials such as photopolymerizable polymer resins to interact effectively with affordable laser light to manufacture products. Unfortunately, when manufacturing products with AM applications, there can be a significant loss in effective properties that are expected of mass-produced parts. Through the layer-by-layer process, designers now have access to formerly unavailable internal volumes. In these now available volumes, architected materials can be made by combining materials of differing properties to produce composite structures that otherwise could not be manufactured.

One of the constraints common to AM materials is the need for rapid and predictable solidification during the processing stage. The solidified material is a fundamental part of how the next layer of liquid-like material can be supported. In thermoplastic extrusion printing, the solid material is rapidly melted at the end of the extruder. As the plastic flows out of the nozzle, the material quickly cools and becomes solid. In material jetting, solidification is also important because the liquid inks are highly sensitive to UV light and the droplets polymerize into solids as soon as they land on the build volume. Stereolithographic (SLA) printing also requires photopolymerizable material to adhere to the build plate rapidly as the laser or light source quickly moves to initial the crosslink process. Without rapid solidification, the geometry of the printed part would not hold and the subsequent layers would not form or adhere. Selective laser melting (SLM) of polymer powder also relies on solidification of the melted powder to hold shape before the next layer of powder and laser heat is applied.

Thermoplastic extrusion is quite popular because of the relative simplicity of the technology and the useful mechanical properties of the material. However, the thermoplastic materials used are susceptible to many environmental factors such as heat and solvents. Due to susceptibility to environmental factors, thermoplastics are not appropriate for use in aerospace or medical applications. Many other polymers, i.e. silicones, possess many of these other properties that make them resistant to chemically and thermally abusive environments. These other polymers can be quite complex and require a higher understanding of processing conditions needed for successful AM.

When evaluating new materials to use with AM, understanding how materials can undergo this rapid solidification is an essential part of developing a repeatable and accurate process. Many common silicones can be cured to a solid with heat or UV light. However, use of these silicones in AM processes would require machines to be specially designed to provide for rapid solidification. A useful subset of silicones have shear-thinning properties that change viscosity depending on the extrusion pressure applied. By controlling the extrusion pressure, self-supporting structures can be printed without inducing a permanent cross-linking reaction. These types of silicones can be integrated into the existing material extrusion printing processes with thermoplastics to leverage the high mechanical properties of thermoplastics and the chemical and biocompatibility properties of the silicone thermoset.

1.2 Motivation, Importance, and Focus

Current research trends for materials development views the cutting edge to be found in the development of composites. Composites utilize the properties of multiple similar or different materials in new combinations to achieve a set of properties improved over the individual components. Some of the best materials developed in the last few decades such as thermoplastics and silicones are prime candidates to design composites around to maximize the given attributes of each. Traditional manufacturing of composites; through mixing or layering, lacks the precision to insert or pattern materials. Additive manufacturing has been documented as a successful technique for patterning materials through controlled extruders in a 3D space. Seven types of AM techniques have been developed for the continuous deposition of layers of different materials ranging from food pastes to metallic powders. To produce multiple material composites with AM, various techniques are acceptable. The aim of the research is to utilize two different techniques; FFF and DIW to process thermoplastics and thermosets into layered composites of a silicone matrix with thermoplastic reinforcement patterns. The results make a good case for demonstrating the effect of dual extruding dissimilar materials of different flow characteristics and mechanical properties have on the overall strength and stiffness of the parts.

1.3 Order of Information in the Thesis

The following chapter will cover a literature review of all related aspects frame this thesis work in Chapter 2. Chapter 3 covers the process development of the printing hardware. Process controls and fundamental optimization are discussed in Chapter 4. Chapter 5 describes the tensile tests of the composite structures and the results of the experiment. Viscosity and shear thinning observations of commercially available silicones are presented in Chapter 6. Finally, the conclusions and future work are discussed in Chapter 7. Additional data are presented in the Appendix.

Chapter 2

Literature Review

2.1 Introduction

Additive manufacturing (AM) is the process of depositing material in a layer-by-layer manner through computer control such that the part produced have thickness in three dimensions. In recent years, AM has been challenging the current manufacturing workflows and methods. Through this layer-by-layer process, designers and engineers have been able to utilize AM to: (1) decrease time to market through rapid prototyping, (2) generate novel designs through nearly unlimited complexity, and (3) integrate new combinations of materials through in situ composite manufacturing[1]. ASTM and ISO categorized AM into seven unique methods for depositing material. The methods are differentiated by feedstock and deposition techniques[2].

Material extrusion has been widely accepted across the world as the most popular method of AM due to the simplicity and low cost of entry. The core principle of material extrusion is taking a feedstock and moving the material through a nozzle. The extrusion force can be applied by electronic motors or pneumatic pistons[3], [4]. The most common subset of material extrusion is fused filament fabrication (FFF) where the feedstock is commonly a spool of thermoplastic filament. The thermoplastic material is liquified by a heated nozzle and extruded into the build volume. Ideal feedstock material needs to be at a viscosity such that the machine can extrude the material in a reasonable timescale where parts can be produced.

A second class of AM is vat photopolymerization. Two vat photopolymerization types are: stereolithography (SLA) and digital light projection (DLP)[5]. In both types, the feed stock is a liquid of light sensitive monomers contained in a tank or tray. Through reflected laser energy or patterned projected light, the light source activates a photoinitiator chemical to start the monomer crosslinking process. Through this one-way crosslinking process, there is a phase change from a liquid to a solid. The feedstock is tuned to specific wavelengths of light to initiate the photopolymer crosslink. The process is favored for the high resolution and accuracy of plastic parts for rapid prototyping as well as a multitude of medical grade materials[6].

Powder bed fusion (PBF) is the third class that uses thermoplastic powder or metal powder and a high intensity layer to fuse the powder together into a solid part [7]. After the first layer of material solidifies, a re-coater blade evenly spreads powder over the build surface to apply material for the next layer. Resolution is dictated by the size of the melt pool to incorporate enough powder particles consistently. Similar to all other AM processes, the stability and accuracy of the end product is highly dependent on the rapid solidification control of the feedstock.

Binder jetting is an AM process that utilizes a similar powder bed and re-coater method but also uses a nozzle to deposit a polymer-based binder to hold the powder together. The binder is very fluid like and is ejected from a nozzle onto the layer of powder. The binder is designed in such a way that it has consistent interaction with the powder bed and quick evaporation of solvents so that the binder can be a solid in a quicker time scale. An advantage with this process is that the binder can be designed to be powder agnostic so that many substances, from metal to ceramic to sugar, can be used. The parts that come out of the print volume are considered unfinished since they need a post process heat treatment to consolidate the powder into a solid material[8].

Directed energy deposition (DED) is an AM process that involves use of laser or electron beam to melt powder onto a build surface. In this process, powder is delivered in a stream out of the nozzle and aimed for the focal point of the energy source. Without the need for a powder bed, the process can be adapted to many different gantries and even industrial arms. With the use of electron beams, the build chamber needs to be under vacuum. DED has been commonly used to make large scale metal structures such as rocket engines as well as assisting in the repair process for damaged cargo ship components[9].

Ink-jetting involves low viscosity inks that are ejected from a nozzle in droplet forms onto a substrate. With piezoelectric or pneumatic activated nozzles, ink jetting can provide a much higher resolution than other AM processes. This high resolution is dependent on the calibrated formation of drops of polymer ink at the nozzle and formulations in the ink to be highly sensitive to UV light. The drop size controls the amount of material per deposition and the light sensitivity controls how the fluid solidifies in the print volume. Use of a series of nozzles allows for the development of unique material gradients involving stiff and elastic polymers[10]. Ink jetting is restricted to very low viscosity inks that usually require some catalyst or light source to rapidly solidify so that the ink drops do not flow into unintended areas

The seventh designated technique of AM is known as sheet lamination. In this method, sheets of feedstock are laid onto a build surface. Each new layer is adhered to the subsequent layer and given a subtractive method to remove excess material[11]. Paper based feedstocks are adhered with glue and trimmed with a razor. Through ultrasonic welding, many types of metal feedstocks can be joined together and trimmed with an engraving or milling operation. Although this is a more wasteful AM prosses with the added subtractive step, the advantage is that the feedstock does not undergo a phase change. By having consistently solid feedstock, the dwell time usually allotted to the rapid phase change in AM is removed and over all print time decreased.

2.2 Fused filament fabrication

As a subset of material extrusion, FFF follows the same core tenants of depositing material through a nozzle opening onto a build volume. However, the nozzle is heated to flow the thermoplastic feedstock. To process the feedstock, the nozzle has to be heated up to the correct temperature range for the solid and usually brittle thermoplastic to melt and flow easily. First developed in the 1980s and commercialized by Stratasys in 1990, FFF has become one of the most commonly used AM methods. The home consumer market dictated development of affordable printers at a desktop scale with open-source technology for personal modification. Current advances in this technology have been to expand the size and speed of these printers[12] allow use in more industrial markets. Such advances can be seen at Oak Ridge National Laboratory with the development of the big area additive manufacturing (BAAM) system that can process carbon fiber filled thermoplastic pellets.

2.3 Thermoplastics

Thermoplastics have been widely used in the FFF AM space. The advantage of these materials is that they can be solid at room temperature and then undergo a phase transformation to a liquid state by applying heat. This phase change from solid to liquid and back to solid from liquid can be done a countless number of times with minimal effect on the overall properties. The material is easy to process from pellets to filament to a 3D print and then, in some cases, recycled by melting down the plastic back into pellets[13]. Thermoplastics were not initially developed for AM but rather developed for traditional plastic manufacturing. Thermoplastics can be seen in mainstream manufacturing for all sorts of devices. The heat dependent flow characteristics are ideal for injection molding. Many of the hard plastics we see around us every day from water bottles to airplane control are manufactured from these thermoplastic materials. As we consider AM as an industrial scale manufacturing technique for making end use parts, the materials used in the AM process have to be up to the challenge. One of the short coming of thermoplastics is the vulnerability to degradation by many common solvents.

2.4 Direct ink writing

Another subset of material extrusion AM is direct ink writing (DIW). The DIW method differs from other subsets of material extrusion because the feedstock inks are usually in a liquid like state and do not need to melted. These inks or pastes can be made of either colloidal, nanoparticle, or organic materials[14]. DIW has been used to make 3D shapes with suspensions of ceramics, metal alloys, polymers, and even edible materials[15]. This technique is one of the most versatile methods to produce 3D prototypes[16]. The extrusion and flow characteristics of these inks determine appropriateness for use in the DIW process. Inks have to be: (1) easy to load into the machine, (2) thick enough to support the weight of the part being printed, and (3) most importantly shear down in viscosity to be an extrudable material within the processing limits of the machine. Materials that possess high viscosities are not readily processable through this extrusion technique. Depending on the feedstock, DIW prints also need to undergo a post processing heat treatment to consolidate the material into final expected mechanical strength[14][17]. DIW is not limited to polymer or ceramic only materials. The materials used just need to meet the aforementioned requirements for material processing. Other materials of interest with similar flow characteristics include food items such as chocolate[18][19] and other condiments[20] to construction materials such as cement[21]. These systems for printing also feature the pneumatic or mechanical extrusion system with a syringe of premixed material for extrusion. However, since many of the feedstock materials retain fluid like properties after extrusion, work is being done to evaluate and optimize printing parameters based on the individual material characteristics. One such work looks at the bridging characteristics of chocolate extrusion through manipulation of federate and temperature of air quench[18]. With such a wide range of available materials for processing, DIW is the best

AM technique for extruding materials with fluid like flow characteristics.

2.5 Silicones

Poly-siloxanes or better known as silicone elastomers, are common materials used in many applications due to the unique chemical, mechanical, thermal, and biocompatible properties. Many silicone products are produced through injection molding due to low cost per part. AM can be leveraged for rapid prototyping of highly custom designs[22].

Although highly useful, the wide variety of silicones has prevented the formation of commonly accepted freeform manufacturing techniques. The solidification mechanisms are highly different from the thermal phase change of thermoplastics used in AM. These mechanisms can include: (1) phase change, (2) solvent evaporation, (3) polymerization, or (4) some combination. The solidification time scale is a constant issue where silicones compete with other thermoplastics for use in processing. Thermosets, like silicones, do not have the rapid liquid to solid phase change as seen in thermoplastics, and therefore, these materials have to be processed in ways that counteract effects from gravitational fluid flow and other self-leveling tendencies [23].

Silicones that are printed are usually two-part “off the shelf” materials that have a level of consistency before being used. Commonly used silicones are also chosen either for ease of mixing, cost per unit, or for the inherent chemical properties relevant to application. Recent research into silicone geometry stability has shown that using silicones with ideal post-processing shear characteristics is equally if not more important than the preprocessing flow characteristics [24]. Because AM technology can be used to print highly complex parts, having reliable materials is a key aspect to the success of the process.

2.6 Silicone extrusion

Silicones possesses nearly ideal soft yet flexible mechanical properties and chemically resistant properties. In many cases, thermoplastic AM is used to rapidly produce a complex mold that can be filled with silicone [25]. Additively manufactured silicone has been used to create unique medical shapes[26] as well as architected soft robotics[27]. Applications include personalized medical devices, one off seals, and innovative soft robotics[23]. The main additive processes that utilize silicones in their feedstocks are: (1) fused filament fabrication (FFF), (2) direct ink writing (DIW), (3) digital light processing (DLP), and (4) vat photopolymerization (VPP). All of these systems utilize a phase transformation of the silicone from a liquid like state to a solid. This change can happen through a number of mechanisms based on the formulation of the silicone. DIW has been a common method to print silicones

Extrusion forces to extrude the materials can be found in pressure-based systems[27] or mechanical-based systems. Pressure systems can deliver higher extrusion forces as well as more consistent extrusion force. With minimal moving parts, the simplicity of pressure systems leads to them being easier to service. However, pressure systems require either a sophisticated regulator or a technician to manually activate and monitor pressure as the viscosity of the material evolves or as the extrusion starts and stops. Geared extruders have more complex parts but can be neatly integrated into the machines that would use the same control board to move the axis motors. Geared extruders are also able to back drive and, with a sufficient seal, can retract material to reduce the deposition of unintended drips and artifacts onto the surfaces. With electronic control, the extrusion force can be digitally programmed to adapt to the changing flow characteristics as the feedstock reservoir depletes.

Printers developed for printing thermosets and more specifically silicones repeat the same construction process. The established work looks at removing the thermoplastic extruder from an existing commercially available FFF printer to be replaced with the silicone extruder[27]–[29]. By solely using one extruder over another, the research has demonstrated repeated successful methods for controlled extrusion of silicones. However, through the design choice, there is no net function or process gain as one material is replaced with another. As composites are becoming more and more used in industry to advance materials, there exists the potential to include both materials into a single printing system so that the machine can produce composite structures of multiple materials with differing polymer mechanisms.

2.7 Composites

Composites are defined as the combination of two or more materials with differing properties that result in a product with more desirable characteristics than the individual materials [30]. Although many composites are used for the combination of mechanical properties, composites are also used for other properties: (1) electrical, (2) chemical, (3) optical, or (4) thermal. Composites are generally defined as either "fiber reinforced" or "particle reinforced" based on the filler material used. Particle reinforced composites are common in industrial manufacturing due to the relative ease of use. The particle is evenly dispersed into the matrix before forming the desired final shape. A very common material used in particle reinforced composites is carbon black, a low cost and strong particle that adds significant mechanical strength evenly to the whole composite[31]. Fiber-reinforced composites involve imbedding a fiber or fibers into the matrix. The resultant mechanical properties of a fiber-reinforced composite structure are largely defined by the strength and modulus of the fiber, the chemical stability of the fiber, the strength of the matrix, and the interface strength between the fiber and the matrix for ideal stress transfer[32]. Fiber-reinforced polymer composites are desired for the higher strength to weight ratio and for ease of manufacturing compared to other non-polymer materials[33]. In this case, the sought-after effect is not a decrease in weight but an increase in strength and stiffness from the addition of the fibers.

2.8 Multi-material printing

Multiple material AM grows from the desire for more complex shapes and novel materials to be incorporated into advanced use cases. With DIW, the standard practice has to add multiple nozzles or extruder for each material to build composite structures for improvement of multiple properties such as mechanical[34] or electrical[35]. With the addition of more print heads, the research trend limits the machines to materials that are behave in relatively similar ways. As seen in work done by Hardin[36], demonstrates dual extrusion of viscoelastic inks that possess thermosetting properties into composites structures out of one nozzle. The research leverages the known fluid control system developed for one of the inks to aid in the extrusion of the other ink. Similarly, other research that works with either thermoplastics or thermosets with dual extrusion utilizes the same type of material for the additional extruders.

The primary aim of this study was to create a high strength 3D printed silicone-based parts that utilized traditional FFF filaments for the increase in strength for aerospace and medical applications where the currently available silicones do not meet the desired mechanical properties for reliable performance. Silicones used for encapsulation of the patterned thermoplastic reinforcement are currently accepted and marketed as aerospace and/or medical grade materials not initially developed for AM. With these new silicones, thermoplastic filament was patterned into the samples to evaluate the strengthening effect of the silicone. With the developed extrusion system, a series of capillary fluid flow measurements can be taken from the net material extruded to generate the settings needed for effective printing parameters of nonoptimized materials.

Over all, this paper provides a solution for a single-step manufacturing for multi-material fabrication of reinforced elastomers through patterning and layering of the materials. Based on commercially available FFF 3D printers and material characterization of shear thinning fluid flow, the system reliably produces multi-material composites with novel reinforcement.

Chapter 3

Direct Ink Writing Process Development

3.1 Introduction

This work looks to document the process of developing an additive manufacturing machine that can manipulate both thermoplastics and thermosetting silicones to produce unique composite materials. The process uses a robust mechanical frame, a developed thermoplastic extruder, and the integration of a precise fluidic dispenser to produce composite materials with desirable strength characteristics.

3.2 3D Printer hardware

The base for the dual extrusion AM machine is a TAZ Lulzbot (Aleph Objects Inc., Loveland, CO). This base was chosen due to the open-source nature of the hardware and software as well as the high rigidity and desktop scale factor. Included in the design of the printer is an "auto bed leveling" function where the thermoplastic nozzle grounds current at four corners of the bed to account for any warps or offsets in the actual frame. The core elements of the thermoplastic extruder, such as the heater and nozzle, were unmodified. The extruder is built from the direct drive Titan Aero design (E3D, Oxford, Oxfordshire, UK) with a 0.5mm inner diameter nozzle.

The thermoset ink extruder was assembled from a high-pressure fluidic extrusion system made by Nordson EFD (Ultimus V, Nordson EFD, Westlake, OH). The system is comprised of a 10 cc polypropylene syringe with a Luer lock thread for accurately dimensioned extrusion tips. The syringe fits into a high-pressure extruder body (HPx High Pressure Dispensing Tool, Nordson EFD, Westlake, OH) that converts pneumatic pressure into physical extrusion force through a piston. The high-pressure extruder is connected through a pneumatic tube into a Nordson Ultimus V pressure regulator. The regulator controls input air of 100 psi and outputs specific pressure through the control interface on the Ultimus V LCD interface. The pressure system is controlled through the I/O port and a 5V signal from the printer thus making a closed-loop automated extrusion system. Through an integrated G-code post-processor in Cura Lulzbot, the pin was automatically signaled on/off when the alternating between thermoplastic extrusion and silicone writing.

To physically integrate the ink extruder with the thermoplastic extruder in the end effector of the printer, a custom bracket was designed. The extruder bracket was extensively iterated upon to find an effective design that allowed placement of the ink extruder as close as possible to the thermoplastic nozzle without interfering with the normal motion of the printer and that minimized any deflection of the nozzle tip to increase accuracy and repeatability of extrusion. These design improvements can be seen in the change from the initial version of the extruder bracket to the final design used. A separate PID controller with a 12V heating band was later added to the end of the thermoset silicone extruder. This heating element had a dedicated power supply and control system. The use of the heating element was to increase the average temperature of the raw material to lower the viscosity to working parameters for the extrusion system.

3D models were developed in Autodesk's Fusion 360 CAD environment and exported as an .STL for slicing and machine code generation. To generate the machine code (known as G-code) for the dual printer, the open-source slicer Cura Lulzbot edition was used. This software converts digital 3D models into simple instructions that direct the print on direction, speed, temperature, and other printing parameters. G-code was unmodified and directly loaded onto the SD memory card in the 3D printer. Figure 1 visualizes the work flow to: (1) generate a 3d model, (2) export into an .STL file (3) slice into machine code, and (4) execute the file on the printer to produce the designed part.

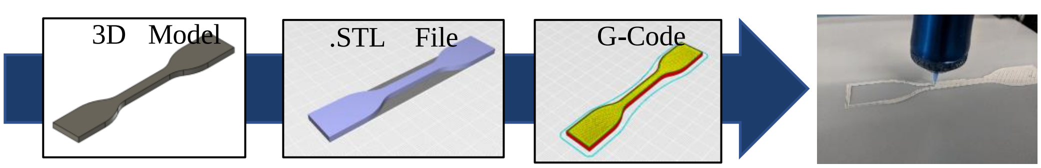

Figure 1 Workflow for printing 3D model

3.3 Silicone extruder arm

One of the challenges in the development of the extrusion system was the mounting of the thermoset ink extruder to the existing hardware. Version 1 of the extruder mount was based on the existing printed geometries used in the thermoplastic extruder hardware. Initial design considerations included ease of manufacturing and ease of integration into the printer. Based primarily on these design considerations, Version 1 had significant drawbacks. Although the initial design, as seen in Figure 1, held the thermoset ink extruder firmly, the extruder was cantilevered far from the thermoplastic extruder. This cantilever led to instability as the vibrations from the movement of the extruder carriage were exaggerated. This initial design also suffered from being too large in the X dimension which caused hardware collisions and limited the overall printing volume. It was important to consider these additional factors in the final design of this single component. Additionally, choosing a design that can be easily printed out of highly durable thermoplastics was also important because the rest of the research hinged on the stability of the mount and the consistency between the two extruders.

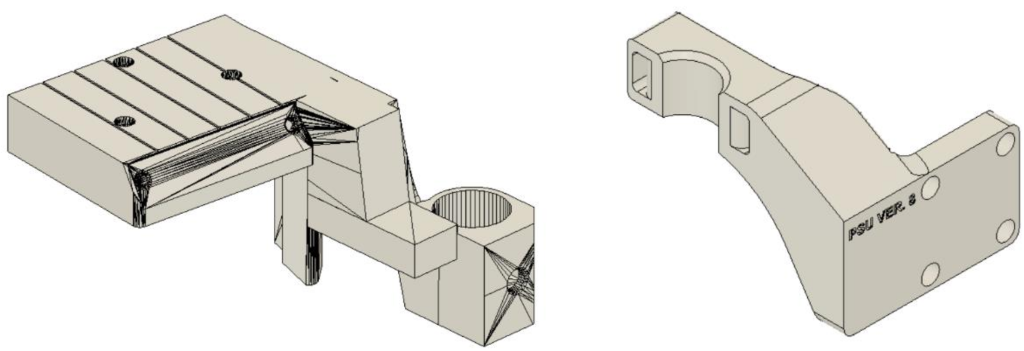

Figure 2 (Left) Version 1 of the silicone extruder and (right) the final version of the silicone extruder

Improvements to the initial design are reflected in the final design seen in Figure 2. To minimize vibrations of the thermoset ink extruder, the fixture location of the extruder mount was relocated to match the mounting holes in the thermoplastic extruder stepper motor. Based on inspection of the default hardware, the motor was chosen because it was identified as the sturdiest component on the extruder assembly without tremendous exposure to heat. To prevent hardware collisions and maximize the build volume, the location of the silicone extruder was moved in front of the extruder carriage and closer to the thermoplastic extruder. The closer the extruders are to each other, the more the print volume of each nozzle can overlap and therefore expand the viable build volume. To predictably design the extruder into the existing hardware, a 3D model was designed for the printer. Figure 3 shows the comparison between the rendered computer model of the hardware and the final assembly used to produce samples.

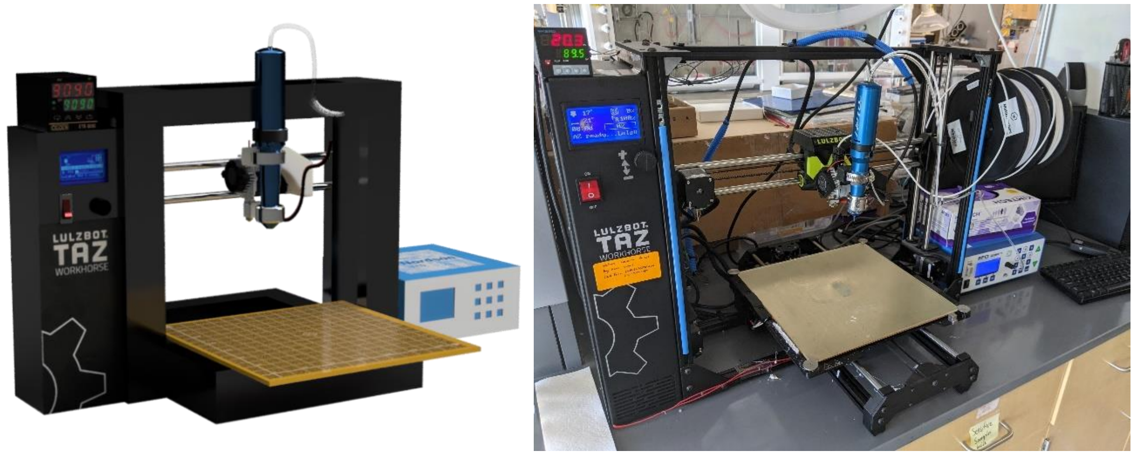

Figure 3 (Left) Render of 3D printer and (right) photo of final 3D printer assembly

Chapter 4

Optimizing Silicone Extrusion Parameters

4.1 Introduction

When working with AM technology, degree of precision is a key element. AM technology can be calibrated to be on par with traditional manufacturing techniques that include injection molding and transfer molding. To understand the precision and processing limits of the dual extrusion machine developed, a set of processing parameters were observed to capitalize on the limits of the AM process.

4.2 Feed rate and flow

When specifically printing with a shear-thinning material, it is imperative that the volumetric flow rate be controlled throughout the printing process. Precision and accuracy in DIW is highly dependent on the similarity between the predicted extrusion rate in the software and observed extrusion rate. The volumetric flow rate can be calibrated for the speed and feed rate of the printer. Assuming a circular bead of material is deposited, the layer height and the bead width would be equal to the inner diameter of the extruder nozzle if the feed rate was set at the correct linear velocity to match the output of flow. To calculate the flow of a material out of a given nozzle, a specific gravity weight of the extruder material over a time duration would need to be known. Using equation 1, the flow rate can be calculated from the mass collected from the nozzle per second divided by the reported density of the silicone.

$$(Vol.\ flow\,rate)Q = \left(\frac{mass}{sec}\right) * \frac{1}{density} \tag{1}$$

Velocity of the nozzle in a linear direction can be defined by equation 2 where the volumetric flow rate, Q, divided by the cross-sectional area of the nozzle. This final value is in mm per second that is input as nozzle speed of the printer.

$$velocity = \frac{Q}{\pi r^2} \tag{2}$$

4.3 Layer height and bead width

Using the nozzle inner diameter and the extrusion pressure into the fluidic dispenser, layer height and line width were calculated to properly calibrate the machine to prevent over or under extrusion of the prints. Over extrusion is defined as the condition when the volumetric flow is greater than the linear feed rate of the nozzle head. Over extrusion results in bead swell around the nozzle. This swelling can cause a catastrophic layer height creep. This creep is not very critical at early layers in the print as the layer height creep might be only 1-2 % out of tolerance. However, as the layers stack up, the tolerance error also stacks up to the point that an over extrusion of 2% in a 0.2mm layer height print would shift the layers up by 0.1 mm by the 25th layer. Under extrusion is defined as a similar but opposite mismatch between volumetric flow rate and linear feed rate where the feed rate exceeds the flow rate of material out of the nozzle. Under extrusion results in a narrower bead of material that is smaller than the expected layer height or line width. A similar under extrusion of 2% at 0.2 mm layer height would shift the layers down by 0.1mm by the 25th layer. Both over extrusion and under extrusion will cause a catastrophic and unreliable failure of printing. Using equation 3, the ideal bead width can be calculated from user specified layer height.

$$bead\ width = \frac{2(r_{nozzle})^2}{(layer\ height)} \tag{3}$$

From these calculations, the dimensions of the print can be input into the slicing software to execute the desired print parameters.

4.4 Bridging and overhang structures

The shear thinning behavior of silicones is a key element to the shape holding and layer supporting feature that makes these materials conducive to the DIW process. Shear thinning is defined as the decrease in viscosity as the material undergoes increased pressure[37]. As the silicone resides in the tube, the material is fairly resistant to flow. As extrusion pressure is applied, the silicone decreases viscosity and flows out of the extruder. After the extrusion pressure is removed (i.e. once the material leaves the nozzle), the silicone returns to a higher viscosity state that can support the next layer of material.

In AM, there often exist geometries that are separated by an unsupported gap in the middle of the deposited layer over which printers are directed to extrude material. Thermoplastic based extrusion printers use a series of cooling fans to cause rapid solidification of the extruded material to stiffen the bead so that it can successfully self-support until the bead is extruded to the other side of the gap. With effective cooling, thermoplastics are able to bridge significant gaps. The distance over which the bead can successfully cross without significant deformation caused by gravity is called “bridging”. Shear thinning materials can achieve a similar amount of bridging with the observed return from low viscosity to high viscosity state.

Overhangs are defined as areas where part of the next added bead of material is offset from the previous bead. Overhang regions can also have severe enough angles to the point where the subsequent bead of material is not completely or even partially supported by the previous layer. Overhangs are typically solved in thermoplastic printing with more rapid solidification by cooling or with the addition of removable support structures. Challenges presented by difficult geometries increase when printing with soft materials that do not have the opportunity to undergo rapid solidification[29].

4.5 Corner Acceleration

In straight features of a printed part, the nozzle moves at a consistent linear speed. Flow rate and linear speed result in deposition of a consistent bead with the desired layer height and line width characteristics. When sharp corners or sudden changes in directions are required, the change in vector is not instantaneous, and the printer needs to decelerate the nozzle. In this instance the flow rate and the nozzle are decoupled from a lack of feedback loop in the system. Due to the controlled constant flow rate of the fluidic extruder, there is an observed over deposition of material in sharp corners in the XY plane. This over deposition results from the deceleration from the print nozzle as the nozzle abruptly changes directions. A strategy to mitigate over extrusion due to constant flow rate is to add fillets and radii to every sharp angle in the XY plane.

4.6 Dual extruded print

Test prints can be used to showcase the effect that careful and accurate calibration and understanding of good process control of the machine can do to promote accurate structures. In Figure 4, a model representing the Penn State Nittany Lion logo[38] was used with high viscosity silicone. This print is made of three layers of material: two layers of silicone and one internal reinforcing layer of nylon thermoplastic. The start and stop integration of the extruder is highlighted as the model has “islands” of geometry. Through the evaluation of the bead formation from the nozzle, the printer is able to evenly and smoothly lay beads of silicone.

Figure 4 (Left) Silicone and thermoplastic composite Nittany Lion and (right) thermoplastic print of Nittany Lion

Chapter 5

Reinforced Thermoset Composite Structures

5.1 Introduction

With the novel multi-material printing demonstrated, the next step was to demonstrate mechanical advantage using rigid thermoplastics patterned as reinforcement inside a silicone bulk material. To evaluate the mechanical strength of thermoplastic and thermosetting silicone composites, a series of tensile bars were printed with a single layer of reinforcing structure or “mesh” surrounded by a layer of thermosetting silicone on each side. This process created a three-layer composite tensile bar that was used to compare the effect that different types of thermoplastics and patterns had on the mechanical strength between the composite structures.

5.2 Silicones

Silicone rubber is an import inorganic polymer in modern manufacturing because of the high thermal stability, elasticity, and in some cases biocompatibility. Silicones are commonly used in manufacturing but it is recognized that pure or unfilled silicone may not have the needed mechanical strength for many applications[39]. To improve the mechanical strength of silicones, composite mixtures of silicone and a secondary material are developed[40].

5.3 Composites

Composites are defined as combinations of two or more materials where the resultant mixture has improved properties over the individual materials. The materials used can fall into the two categories of matrix or reinforcement. The matrix is the build material that holds or binds the reinforcement together. Composite reinforcement types are categorized as fiber or dispersant reinforcement[41]. Dispersants in composites are usually a fine powder or chopped material mixed into the bulk material before the fabrication of the desired geometry. One advantage of this type of reinforcement is that the additive can be universally dispersed across the bulk material. Even dispersant distribution is dependent on the processing but a highly mixed composite would show direction agnostic strength. Dispersants have been commonly used in many silicones and other thermoset materials to modify strength or flow characteristics[42]. The use of carbon black into rubber for increasing the life of car tires is such an example [31].

Fiber based reinforcements are used in higher strength composites due to the purposeful alignment of large fibers along the direction of stress. Fibers are usually chosen for higher tensile strength. Assuming perfect adhesion, fibers bear the majority of the load which is transferred through the bulk material. The net effect is that the over composite has the stiffness of the fibers with the ultimate strength of the bulk material. Ply orientations, fiber volume fraction, number of layers, stacking sequence, material, and layer thickness are all parameters that have high contributions to the resultant properties of the composite [43].

5.4 Methods and materials

Materials used to produce the three-layer composites are (1) nylon, PETG, and ABS thermoplastic filament intended for use in FFF 3D printers and (2) PrimeTech Batch AMS3302H (PrimeTech Silicones, Inc., Riverside, CA) single part peroxide curing silicone intended for industrial transfer molding of aerospace parts. Using both materials was key to demonstrating and understanding the relationship between the common material in AM and the common material used in the molding industry.

Two sets of samples were generated. The first set of samples maintains a consistent mesh pattern and the materials used in the pattern are differed to determine tensile strength of the reinforcement fiber. The second set of samples focuses on one thermoplastic with a variety of mesh patterns to determine the effect of patterns on the mechanical properties in printed silicone composites.

Sample set one is a three-layer composite with a 0°/90° grid thermoplastic reinforcement pattern where the material beads are deposited along the pull direction and perpendicular to the pull direction. 0°/90° grid refers to the orientation angles of the lines in the mesh pattern. 0 degrees represents along the axis of tension and the other is 90 degrees offset of the first lines. This pattern was printed with 20 % infill and 30 % infill densities. Samples were modeled off of the Type I ASTM D412 tensile bar standard for elastomer testing. Each thermoplastic has five samples per infill percentage for a total of thirty samples for the first sample set. Destructive testing was performed on an Instron load frame at a rate of 500 mm/min until full failure. Force and extension data were taken from the load cell and normalized for cross sectional area for each sample to achieve stress versus strain data for the tested tensile bars.

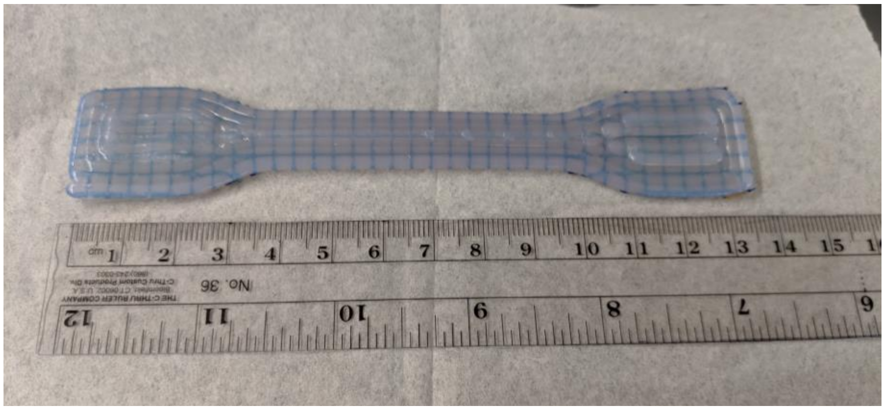

Figure 5 Tensile bar of PETG 20% grid with silicone

Sample set two used the same nylon material from sample set one with a variety of infill patterns. Infill patterns were generated from the Cura Lulzbot Edition slicing software. The patterns generated are seen in Table 1. Infill percentage and, therefore, composite material volume ratio was kept at the same 20% for each of the different mesh designs.

Table 1 Reinforcement mesh patterns

45°/45° Grid	**Triangles**	**Triangles (rotated 90°)**	**Octet 0°/90°**
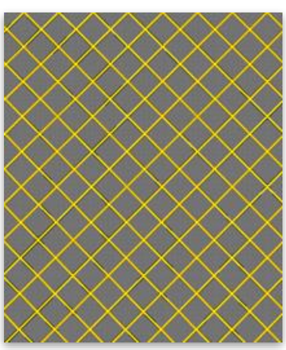	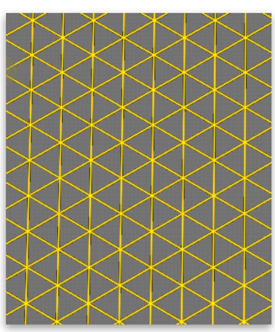	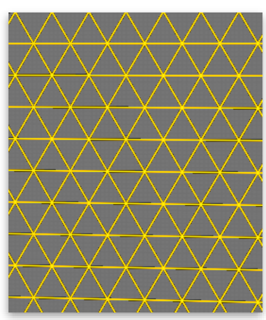	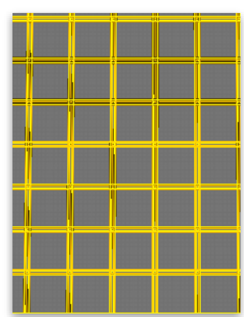
0°/20°/340° Grid	**Tri-Hex**	**Tri-Hex (rotated**	

		90°)
	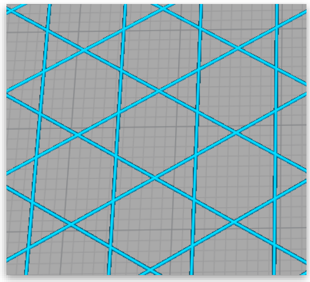	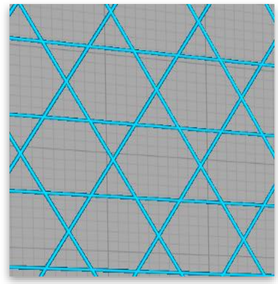

5.5 Results and discussion

5.5.1 Sample set 1: thermoplastic composites

Figure 6 below shows the tensile modulus between the different types of thermoplastics in the three-layer composite sample. Based on the ultimate tensile strength (UTS) of the samples, there is not distinct difference between the materials in the composite structure. This UTS is considered to be the UTS of the silicone used in the three-layer composite structure. Through the testing, there is a point where the reinforcement is fully broken, and the load is transferred to the silicone matrix.

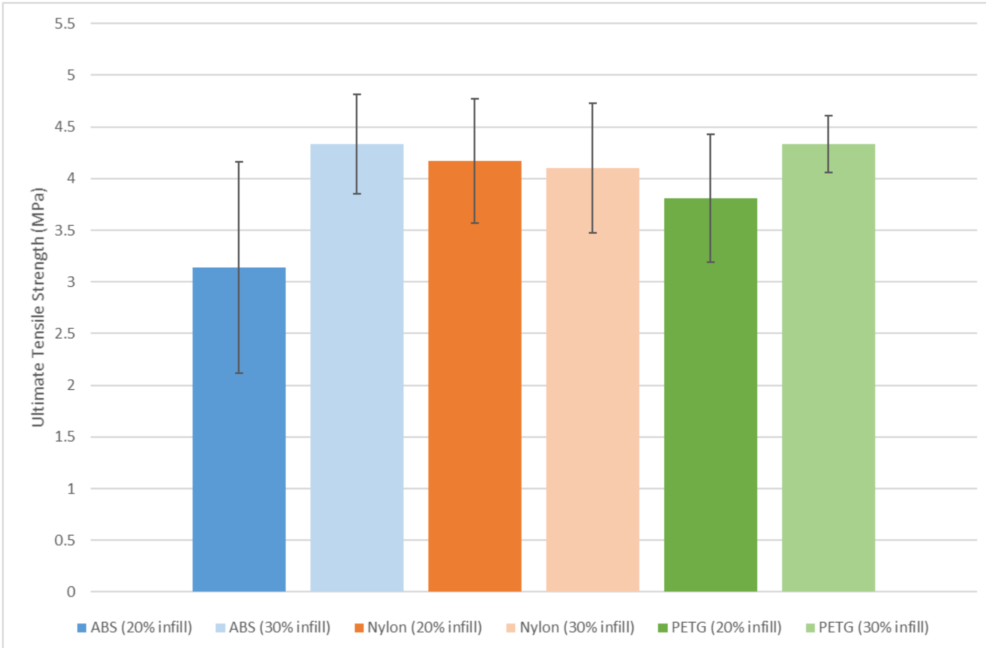

Figure 6 UTS of 3-layer composites with different thermoplastic meshes

In figure 7, the Young's modulus for the first set of samples is presented. Modulus is calculated on the initial linear region of the stress versus strain. Here we can see that PETG contributes to the highest initial stiffness of the three-layer composite. There is also a noticeable correlation between increase in infill density increase in the stiffness of the samples.

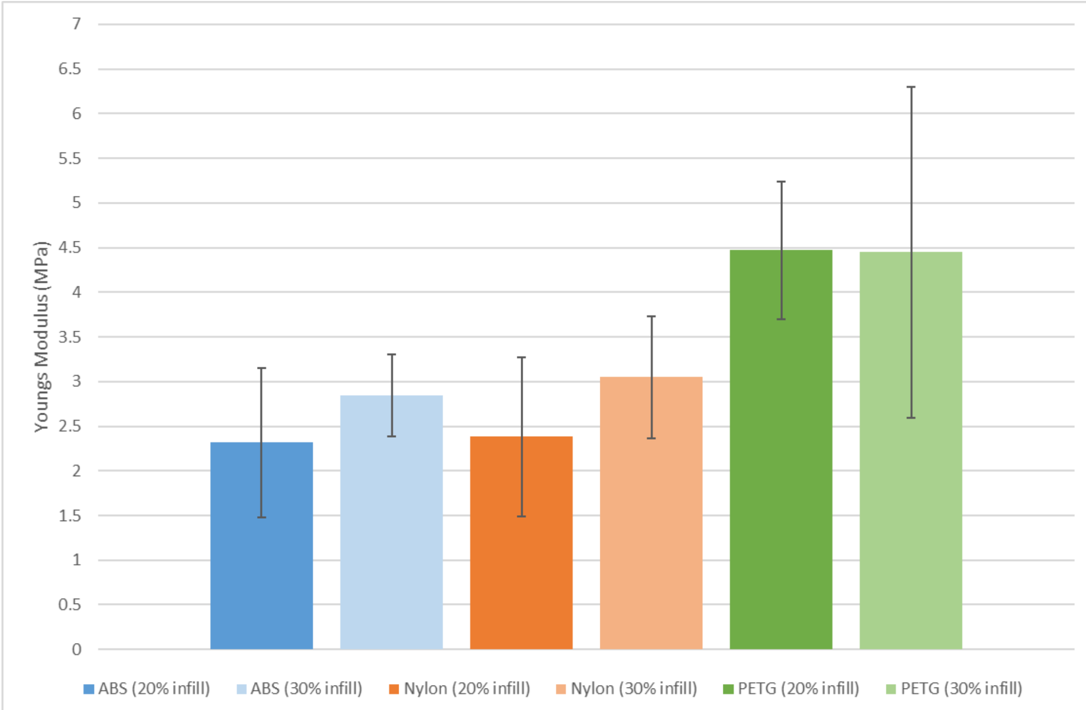

Figure 7 Young's Modulus of 3-layer composites with different thermoplastic meshes

Figure 8 presents the stress versus strain curves of the samples tested. From these graphs, there are two stages of mechanical failure. The two stages are defined by the difference in slope of the stress versus strain curve. The first stage happens at the initial low strain and high stress. In this region, the slope is very steep similar to the pattern observed in homogenous brittle thermoplastics. It is assumed that the reinforcing mesh is bearing the load of the tensile test. When the slope transitions, the mesh has yielded and undergone brittle failure. At this second stage of mechanical failure, the stress versus strain curve presents a more elastic behavior until the silicone reaches the respective UTS. Variation in the UTS between samples can be attributed to destruction of the internal mesh fracturing into shards of sharp plastic that are moved through and damaged the silicone matrix while elastically stretching.

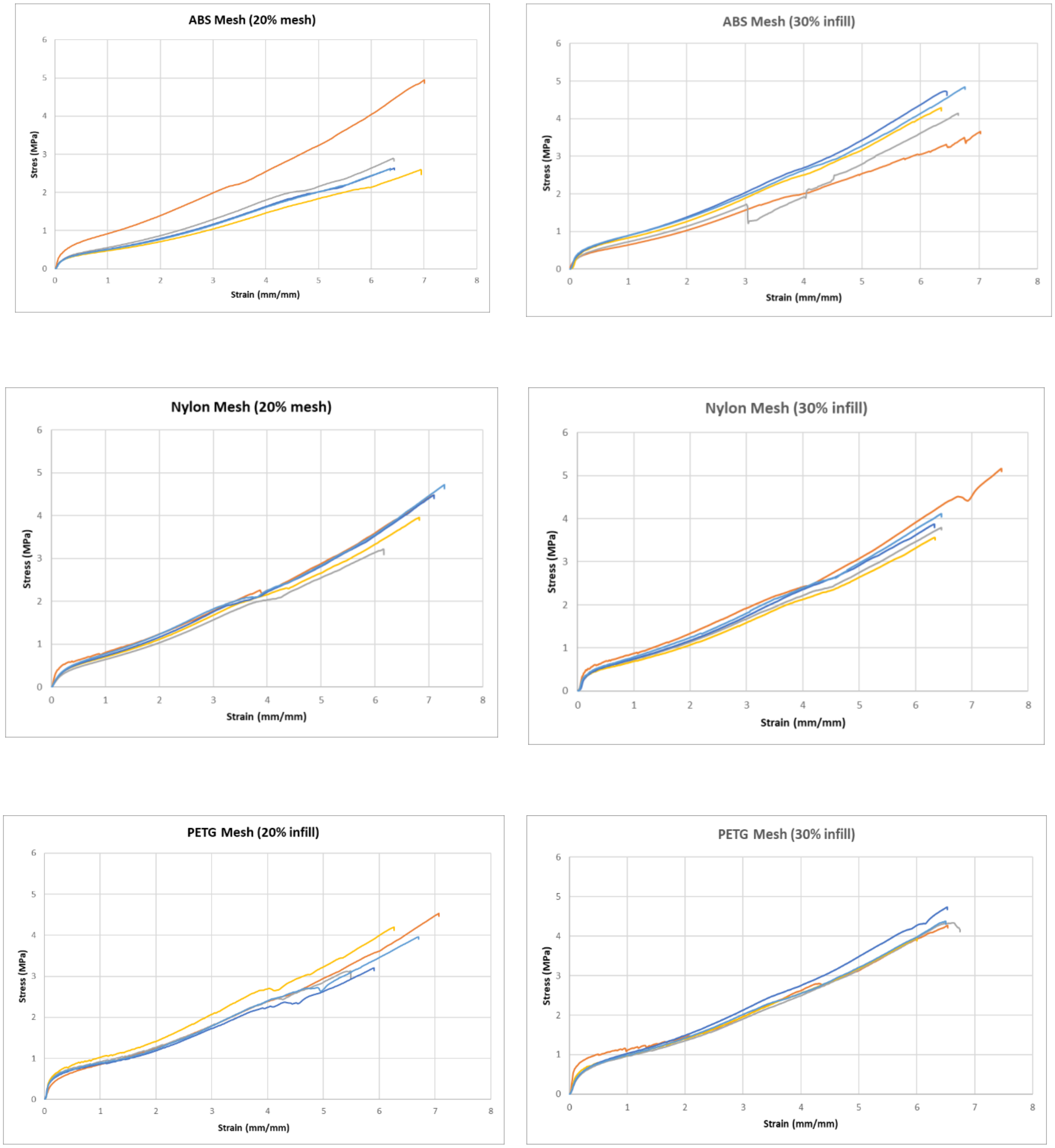

Figure 8 Stress vs strain graphs of mesh reinforcements for different thermoplastics

5.5.2 Sample set 2: patterned composites

Figure 9 visualizes the UTS of the different patterns of meshes with controlled material and infill percentage. Here, we see that the 45°/45° grid, triangles, and 90° rotated triangles, have a lower UTS than the other four types. We also see that these types also have a lower average UTS in the first set of samples. This drop in UTS could be attributed to the destruction in the mesh.

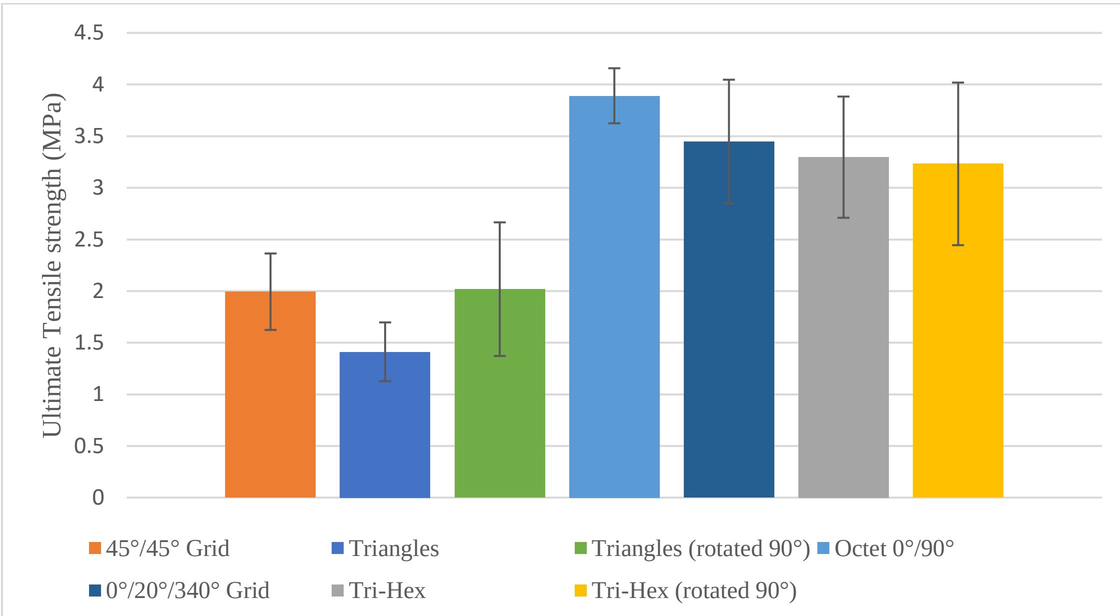

Figure 9 UTS of different mesh patterns

Figure 10 compares the Young's modulus of the different patterns used in this section. The modulus is calculated based on the initial linear region of the stress versus strain curve. Each of the meshes contribute to an increase in stiffness in the modulus region. There is an observed higher modulus in the 0°/20°/340° mesh reinforced composites. This result can be attributed to having a higher degree of reinforcement fibers in the tensile direction. The UTS values are consistent with or lower than the values found in the first samples set demonstrating that certain patterns have no effect on the UTS or negatively impact the final strength of the matrix. The patterns that exhibited a decrease in the UTS did not have as many print lines in the tensile direction and therefor the mesh patterns that failed earlier in the tensile testing. The early failure leads the mesh fragments to negatively affect and destroy the integrity of the silicone matrix.

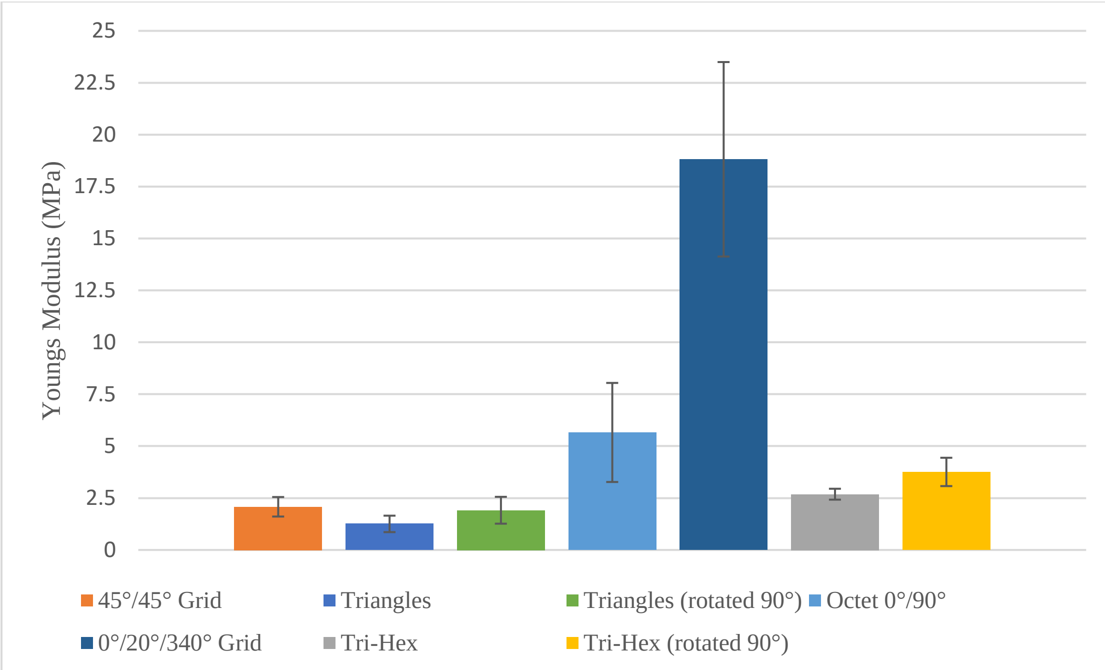

Figure 10 Young's modulus for different mesh patterns

Figure 11 displays the stress versus strain curves for the tested samples. In these samples, there is a distinctive two phases of mechanical failure. The phases resemble the unique mechanical stiffness found in the composite structures in the first set of samples. The first phase is defined by the steep slope in the stress versus strain curve. In this phase, the composite structure is dominated by the patterned mesh reinforcement. As the slope dramatically changes and to a more level slope, the mesh undergoes brittle failure. After the brittle failure, the second phase comprises of the elastic like stress versus strain behavior that is common to silicone elastomers. The 0°/20°/340° grid greatly outperformed the other meshes in stiffness because of the highest number of print lines in the tensile direction.

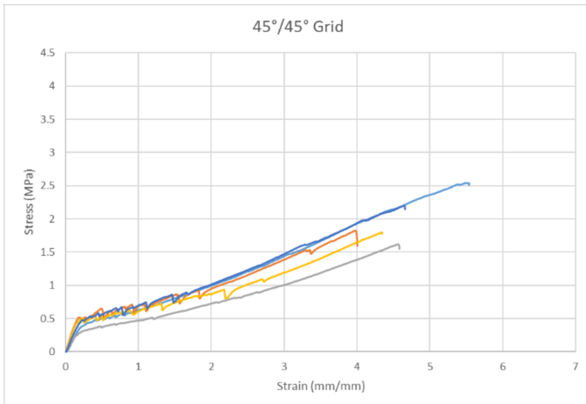
45°/45° Grid
Stress (MPa)
Strain (mm/mm)

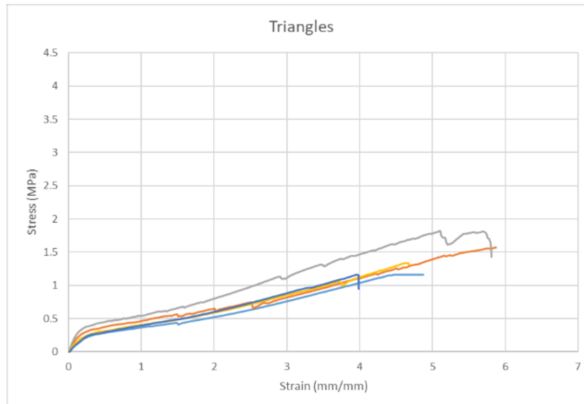
Triangles
Stress (MPa)
Strain (mm/mm)


Triangles (rotated 90°)
Stress (MPa)
Strain (mm/mm)


Octet 0°/90°
Stress (MPa)
Strain (mm/mm)

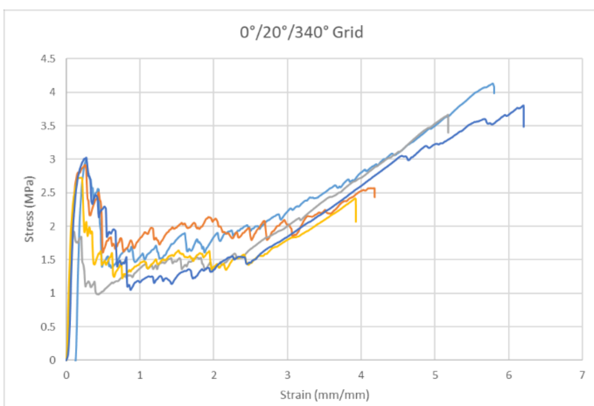
0°/20°/340° Grid
Stress (MPa)
Strain (mm/mm)

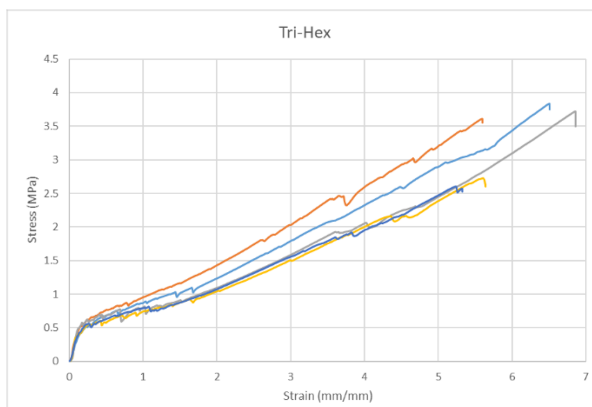
Tri-Hex
Stress (MPa)
Strain (mm/mm)

Figure 11 Stress vs strain graphs of different mesh patterns

5.5 Conclusions

The combination of highly elastic silicone with brittle and stiff thermoplastics resulted in unique combination of mechanical properties. The results of the different samples lead to a unique set of stress strain behavior. The majority of the samples exhibit a high initial stiffness that is mainly dominated by the thermoplastic material. Once the thermoplastic mesh structure fails, the stress level in the sample falls, and the bulk silicone material elastically deforms under the load of the tensile force. The initial stiffness of the composite is reliant on the type of thermoplastic and the pattern in which the material is printed into the silicone matrix.

In the first set of samples, there was an observed two-phase mechanical behavior. In the first phase, the thermoplastic mesh dominates the curve until start of the second phase at the yield point where the curve changes to a more shallow and elastic behavior consistent with the silicone matrix. The UTS of the samples was found to be relatively similar across both (1) the thermoplastics and (2) the infill percentages demonstrating that at the final failure of the sample, the silicone matrix was consistently supporting the majority of the load. Among the different samples, the stiffness or Young's modulus varied between the thermoplastics and infill percentages. Using a consistent mesh pattern, the stiffest composite was the combination of 30% infill and PETG. Increasing the infill density of the pattern results in an increase in stiffness for each thermoplastic. Thermoplastic selection has a distinct impact on the initial stiffness of the composite structure.

The second set of samples is based on the nylon material with variable mesh patterns. Similarly, the samples were able to show a two-phase mechanical failure with an initial high stiffness phase dominated by the thermoplastic mesh and then a secondary phase of elastic elongation after the mesh failure. It was also observed that the more fiber in the tensile direction, the higher the initial stiffness of the three-layer composite. Patterns that were significantly weaker, such as Triangles and 45°/45° Grid, have a much lower quantity of print lines in the tensile direction compared to Octet 0°/90° and 0°/20°/340° Grid. The brittle failure of the mesh contributes to a decrease in the UTS of the composite because the mesh breaks into shards that cause damage to the matrix as the silicone elongates. This self-destruction effect is more present in the weaker mesh patterns that failed earlier in the tensile test. Mesh reinforcement patterns can greatly increase the stiffness of silicone and thermoplastic composites. Non-ideal mesh patterns can negatively affect the mechanical integrity of the matrix.

Chapter 6

Study of Silicone Extrusion for DIW

6.1 Introduction

In this chapter, work outlines a stepped approach to use the extrusion system used for DIW of silicones to characterize the apparent rheological properties of multiple silicones. The materials will be compared to each other by degree of shear thinning and by return to stable solid shape. Higher degrees of shear thinning allow for faster print times and smaller nozzle sizes as well as improved shape holding when extrusion forces are removed from the material.

Additive manufacturing in all forms relies on the rapid solidification of the mobile feed stock into a solid part in order to adhere or support the next print layer. Whether the deposited material is metal powder, concrete, or plastic filament, successful printing requires accurate and rapid transition from a liquid like flow into a structurally solid state to support the next print layer. In traditional thermoplastic extrusion, the phase change to a flow state is induced by adding thermal energy. The thermoplastic transitions to a glass like or melted state where the viscosity is sufficiently low to flow out of the small nozzle diameter at a controlled rate. The controlled rate is a key element for adding the computer software in sending machine code that yields reliable results. After the melted plastic leaves the nozzle, the thermoplastic cools either passively with the environment or actively with the help of directed cooling fans to quickly return the plastic to a solid state. This solid-state change is critical for ensuring that accurate geometries can be printed but it is not without limitations. The phase change for some thermoplastics can lead to thermal gradients that can cause delamination and warping of the plastic as the plastic cools unevenly.

For thermoset materials that exhibit only one chemical phase change, the material is usually printed while still liquid. Ideal DIW extrusion materials have non-Newtonian shear thinning properties. Shear thinning is the decrease in viscosity as force is applied to the material. Some common materials that exhibit shear thinning properties include toothpaste and ketchup. Previous work has established that shear thinning is an important property for DIW feedstocks. Shear thinning materials are useful for printing at high flow rate with low viscosity, and then once extruded and extrusion pressure is eliminated, the material solidifies to hold shape to support the next layer of material.

6.2 Silicone evaluation

To evenly control the extrusion of differing silicones, a high pressure and high accuracy fluid dispenser was used. Built by Nordson EFD, the dispensing technology offers high accuracy as well as a digitally programable dispensing controller. The system also using quick change 10 cc syringe barrels which allows materials to be isolated from each other without risk of cross contamination in the same system.

Silicones evaluated in this process are listed in Table 2 along with relevant properties that are deemed important to the processing of the silicone. SE-1700, manufactured by Dow, is a well-known two-part liquid catalyst and base heat addition-curing silicone used in similar 3D printing techniques. Evolv3D LC-3335, manufactured by Dow, is a two-part platinum curing silicone developed specifically for printing. Silastic Type A, manufactured by Dow Corning, is a room temperature vulcanization (RTV) single part silicone that is rated for medical applications. Silastic 7-4860, manufactured by Dow Corning, is another medical grade silicone made from two parts in a 1:1 ratio of A and B to initiate a platinum-based cure. Liveo C6-770, manufactured by DuPont, is a similar 1:1 ratio of A and B parts.

Table 2 Silicones used for flow characterization

Silicone	**Manufacturer**	**Specific Gravity**	**Cure Mechanism**	**Cure Conditions**
DOWSIL™ SE-1700	Dow	1.13	10:1 Base/Catalyst	30 min @ 150°C
Evolv3D LC-3335	Dow	1.12	A/B Platinum cure	10 min @120°C
Silastic Type A	Dow Corning	1.06	RTV	24-96 hours
Silastic 7-4860	Dow Corning	1.10	A/B Platinum cure	<1 hour @ 140°C
Liveo C6-770	DuPont	1.14	A/B Platinum cure	<30 min @ 120°C

Data taken from respective technical data sheets [44]–[48]

6.3 Methods

To collect capillary viscometry measurement data on the differing silicones, the DIW extrusion set up was programed to accurately dispense material at 3 intervals of 5 seconds at increasing extrusion pressures. The silicones were mixed in accordance with their respective technical data sheet and loaded into 10cc syringe barrels for use in the Ultimus V with the HPx high pressure extruder (Nordson EFD, Westlake, OH). The amount of material dispensed was massed and recorded as a base for comparison. Based on the reported density for the materials in the respective technical data sheet and the diameter of the nozzle, volumetric flow rate was calculated for each silicone for the variable extrusion pressures. The extrusion is pushed through a standardized blue 0.41 mm inner diameter tapered polypropylene nozzle (Nordson EFD, Westlake, OH). In practice, using highly tapered nozzles induced more shear thinning for higher throughput of material at a similar extrusion pressure. Shear stress can be calculated by equation 4. In this equation, pressure drop after the nozzle is noted by "ΔP", radius of the nozzle is represented by "R", and the length of the capillary nozzle is represented by "L".

$$\tau_w = \frac{\Delta PR}{2L} \tag{4}$$

Shear rate is calculated by equation 5. In this equation, volumetric flow rate collected from the nozzle is denoted by "Q" and the inner radius of the nozzle used is denoted by "R".

$$\gamma_{Newt} = \frac{4Q}{\pi R^3} \tag{5}$$

Apparent viscosity (see equation 6) is calculated by the plotting of the shear stress over the shear rate.

$$\eta_{app} = \frac{\tau_w}{\gamma_w} \tag{6}$$

The results of the flow measurements can be seen in figure 12. In this figure the linear extrusion speed of the nozzle is plotted versus the input pressure of the Nordson pressure box into the silicone extrusion system. As the pressure increases, the flow rate of the nozzle increases to match the output volume to maintain a consistent bead dimension. Notably, the linear extrusion speed exponentially increases as a result of a constant increase in the extrusion pressure.

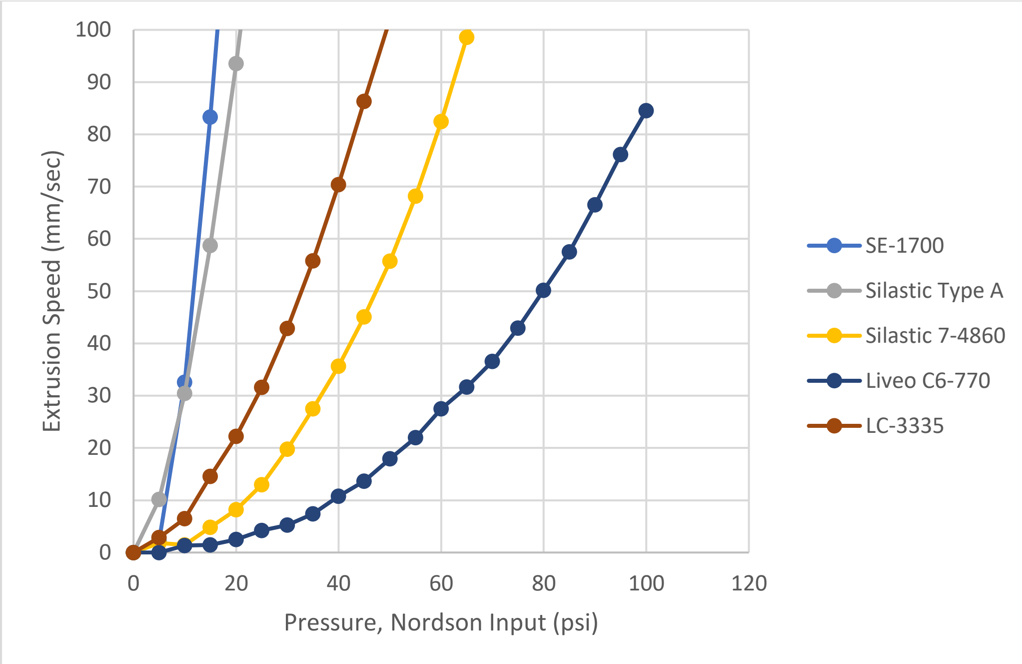

Figure 12 Extrusion speed of the nozzle vs pressure for commercially available silicones

In figure 13, the shear rate versus the shear stress is plotted for the silicones. This graph shows that as the shear rate increases, shear stress exponentially increases. Silicones that show rapid increases in shear stress over low shear rates are silicones that have ideal shear thinning potential for extrusion printing because the silicone is highly resistant to flow with near zero shear rate. Liveo C6-770 shows the steepest increase in shear stress as shear rate increases. The closer the curve is to the shear rate axis, the more fluid like the silicone is with and without extrusion pressure. SE-1700 is the most fluid like state of the silicone.

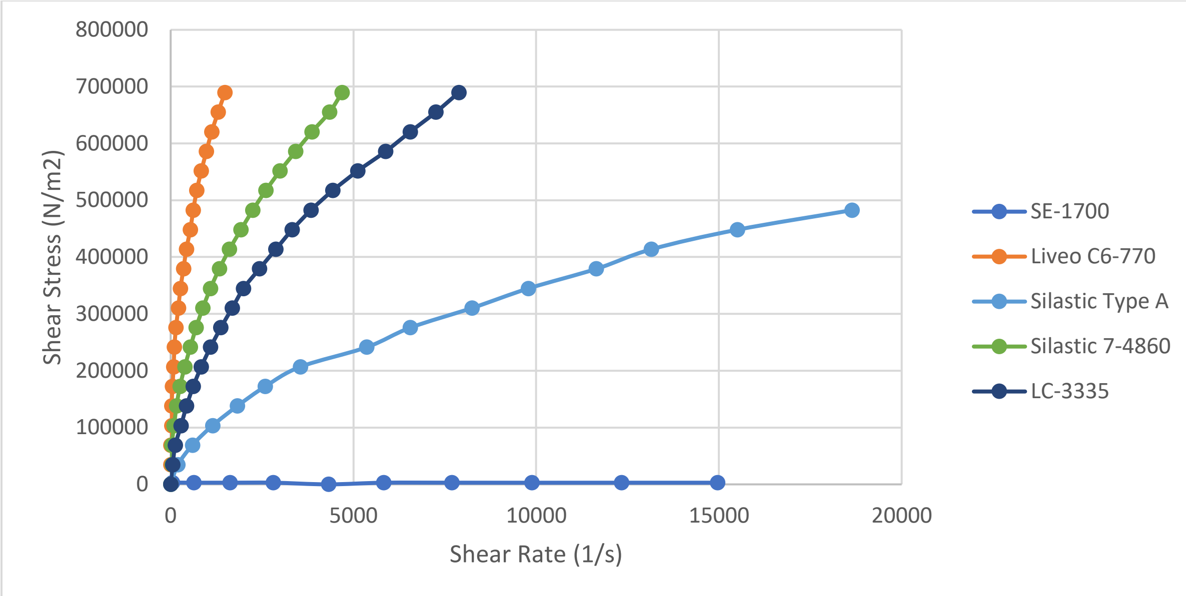

Figure 13 Shear stress vs shear rate for commercially available silicones

Figure 14 shows that as the shear rate increases for the silicones, apparent viscosity drops dramatically. The material with the highest difference in the viscosity is the Liveo C6-770. This silicone exerts the high viscosity under minimal shear and, as the shear increases, the viscosity drops to a processable viscosity that is similar to other printable silicones.

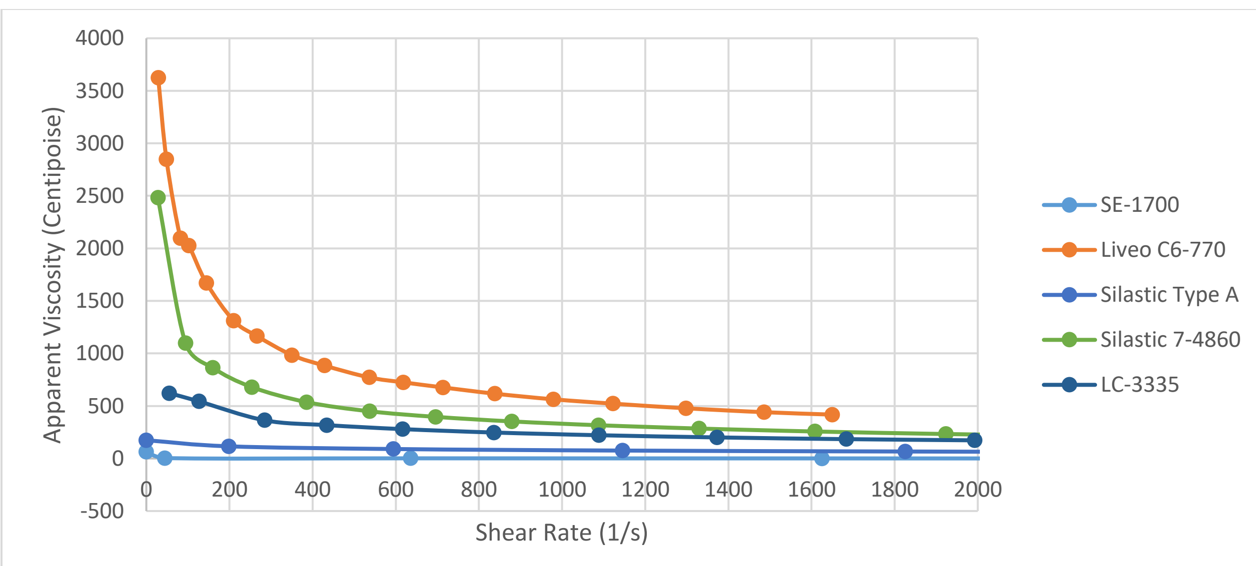

Figure 14 Apparent viscosity vs shear rate for commercially available silicones

6.4 Results and discussion

Based on the resulting calculations, the materials that perform the most consistently in the DIW process have (1) a long working time from initial mixing and (2) have the potential to shear thin down to a very low viscosity under pressure but then return to a high viscosity when pressure is removed to support the addition of new layers of material. A commonly used silicone, SE-1700, has been used in many research papers and served as the comparison point for DIW printing of silicones. SE-1700 is a great silicone for printing fast with a high through put of material. However, Liveo C6-770 does not shear down to as low of a viscosity but the difference between minimal and maximum shear indicates that this silicone has the best shape holding. The other silicones fill out the range of flow between the highly fluid like and the high shear thinning silicones.

6.5 Conclusions

Based on the data collected, the best silicone for DIW possess the following characteristics: (1) loadable into printing syringes, (2) large difference in viscosity between zero shear stress and high shear stress, (3) viscosity with in processing window under high shear stress. Although the silicones may have similar densities, the rheological properties need to be evaluated on a case-by-case basis for individual DIW machines. Testing with the DIW extruder to be used for part printing can be useful to understanding how the silicones and other DIW inks respond to the processing conditions unique to the machine.

Chapter 7

Conclusions and Future Work

Composite AM is a developing area of innovation in which structures of nearly unlimited complexity can be designed and produced. However, composite development is currently limited by the short list of materials that are available for use in AM. Silicone is an interesting material for use in AM because the material possesses different properties than other commonly used polymers. DIW was an effective AM technique to process silicone simultaneously with material extrusion of thermoplastic filament. Current multi-material AM focuses on the extrusion of materials that have similar flow characteristics or other similar processing conditions. The main aim of the research was to develop a single step manufacturing platform from which dissimilar thermoplastic and thermoset materials could be processed into specific reinforced elastomer composites. The unlimited complexity and inner layer access inherent to AM allows for the process to become further elaborate with the reinforcing technique such that multiple patterns are able to be rapidly prototyped and tested. From this research, it has been demonstrated that dual extrusion 3D printing of thermoplastic and thermoset composites can be: (1) done with a relative reliability and accuracy, (2) used to make mechanically stiff composites, (3) improved with ideal flowing materials for the process. The printing success is highly dependent on the optimized integration of a high precision fluidic dispenser and a developed thermoplastic extruder. With a reliable composite AM system, a series of three-layer structures were tested to show how different thermoplastics and patterns of reinforcement meshes improve the initial stiffness of the silicone. It was observed that the mesh was limited to the yield strength of the thermoplastic and could not match the elongation of the silicone through the tensile test. Through this work, ideal silicones possess flow characteristics of high viscosity under low stress and low viscosity under high stress. These flow characteristics allows for better geometry accuracy and shape holding during the printing process.

The inclusion of already processable thermoplastics has been demonstrated to be influential in increasing the stiffness of the composite. Literature shows that when looking at printing silicones, the established commercially available printer gantry systems are commonly used but the thermoplastic extruders are quickly removed from the printers for single material processing.

Rather than replace one extruder for another, this work builds on existing technology to demonstrate the feasibility of multi-material composite printing with two different polymer systems. From the process development, adding stiff thermoplastics greatly increases the stiffness of the silicones which expands the useable range of conditions where silicones can be used.

From the viscosity flow tests of silicones, it is apparent that defined data of the silicones cannot determine the rheological behavior of the material as it flows out of the nozzle under load. Differences in proprietary blends of commercially available silicones affect the near zero shear viscosity and the rate at which the viscosity shear thins during extrusion.

Future work with this technology may be to develop predictive computational models of the dual material composite structures. Utilizing the bulk properties of the thermoplastics and silicone, the computer model would be able to assist in theoretically predicting the strength of the composite as well as aid researchers in understanding the adhesion between the thermoplastic mesh and the silicone. Other areas of future work could include but are not limited to increasing the number of tested silicones and other shear thinning thermosets as well as developing the model to predict and compare the zero-shear behavior of the silicones. The zero shear would be a critical comparison value to gauge the inherent resistant to flow the material has under minimal forces such as on the print bed. Thermosets are a large category of polymers with a wide array of physical and chemical properties. With more tested materials, the combination of composites can be increased.

References

[1] T. D. Ngo, A. Kashani, G. Imbalzano, K. T. Q. Nguyen, and D. Hui, "Additive manufacturing (3D printing): A review of materials, methods, applications and challenges," *Compos. Part B Eng.*, vol. 143, no. February, pp. 172–196, 2018, doi: 10.1016/j.compositesb.2018.02.012.

[2] N. Shahrubudin, T. C. Lee, and R. Ramlan, "An overview on 3D printing technology: Technological, materials, and applications," *Procedia Manuf.*, vol. 35, pp. 1286–1296, 2019, doi: 10.1016/j.promfg.2019.06.089.

[3] C. F. Revelo and H. A. Colorado, "3D printing of kaolinite clay ceramics using the Direct Ink Writing (DIW) technique," *Ceram. Int.*, vol. 44, no. 5, pp. 5673–5682, 2018, doi: 10.1016/j.ceramint.2017.12.219.

[4] F. B. Coulter and A. Ianakiev, "4D Printing Inflatable Silicone Structures," *3D Print. Addit. Manuf.*, vol. 2, no. 3, pp. 140–144, 2015, doi: 10.1089/3dp.2015.0017.

[5] M. Pagac *et al.*, "A review of vat photopolymerization technology: Materials, applications, challenges, and future trends of 3d printing," *Polymers (Basel).*, vol. 13, no. 4, pp. 1–20, 2021, doi: 10.3390/polym13040598.

[6] R. E. Rebong, K. T. Stewart, A. Utreja, and A. A. Ghoneima, "Accuracy of three-dimensional dental resin models created by fused deposition modeling, stereolithography, and Polyjet prototype technologies: A comparative study," *Angle Orthod.*, vol. 88, no. 3, pp. 363–369, 2018, doi: 10.2319/071117-460.1.

[7] S. Vock, B. Klöden, A. Kirchner, T. Weißgärber, and B. Kieback, "Powders for powder bed fusion: a review," *Prog. Addit. Manuf.*, vol. 4, no. 4, pp. 383–397, 2019, doi: 10.1007/s40964-019-00078-6.

[8] M. Ziaee and N. B. Crane, "Binder jetting: A review of process, materials, and methods," *Addit. Manuf.*, vol. 28, no. June, pp. 781–801, 2019, doi: 10.1016/j.addma.2019.05.031.

[9] A. Saboori, A. Aversa, G. Marchese, S. Biamino, M. Lombardi, and P. Fino, "Application

of directed energy deposition-based additive manufacturing in repair,” *Applied Sciences (Switzerland)*, vol. 9, no. 16. MDPI AG, p. 3316, Aug. 01, 2019, doi: 10.3390/app9163316.

[10] M. Müller, Q. U. Huynh, E. Uhlmann, and M. H. Wagner, “Study of inkjet printing as additive manufacturing process for gradient polyurethane material,” *Prod. Eng.*, vol. 8, no. 1–2, pp. 25–32, 2014, doi: 10.1007/s11740-013-0504-0.

[11] C. M. Thakar, S. P. Deshmukh, and T. A. Mulla, “A Review on Selective Depostion Lamination 3D Printing Technique,” *Int. J. Adv. Sci. Res.*, vol. 4, no. 8, pp. 7–11, 2020.

[12] B. Brenken, E. Barocio, A. Favaloro, V. Kunc, and R. B. Pipes, “Fused filament fabrication of fiber-reinforced polymers: A review,” *Addit. Manuf.*, vol. 21, no. February, pp. 1–16, 2018, doi: 10.1016/j.addma.2018.01.002.

[13] J. Pakkanen, D. Manfredi, P. Minetola, and L. Iuliano, “About the use of recycled or biodegradable filaments for sustainability of 3D printing: State of the art and research opportunities,” *Smart Innov. Syst. Technol.*, vol. 68, pp. 776–785, 2017, doi: 10.1007/978-3-319-57078-5_73.

[14] J. A. Lewis, “Direct ink writing of 3D functional materials,” *Adv. Funct. Mater.*, vol. 16, no. 17, pp. 2193–2204, 2006, doi: 10.1002/adfm.200600434.

[15] K. Fu *et al.*, “Graphene Oxide-Based Electrode Inks for 3D-Printed Lithium-Ion Batteries,” *Adv. Mater.*, vol. 28, no. 13, pp. 2587–2594, 2016, doi: 10.1002/adma.201505391.

[16] R. D. Farahani, M. Dubé, and D. Therriault, “Three-Dimensional Printing of Multifunctional Nanocomposites: Manufacturing Techniques and Applications,” *Adv. Mater.*, vol. 28, no. 28, pp. 5794–5821, 2016, doi: 10.1002/adma.201506215.

[17] N. W. S. Pinargote, A. Smirnov, N. Peretyagin, A. Seleznev, and P. Peretyagin, “Direct ink writing technology (3d printing) of graphene-based ceramic nanocomposites: A review,” *Nanomaterials*, vol. 10, no. 7, pp. 1–48, 2020, doi: 10.3390/nano10071300.

[18] M. Lanaro *et al.*, “3D printing complex chocolate objects: Platform design, optimization and evaluation,” *J. Food Eng.*, vol. 215, pp. 13–22, 2017, doi:

10.1016/j.jfoodeng.2017.06.029.

[19] R. Karyappa and M. Hashimoto, "Chocolate-based Ink Three-dimensional Printing (Ci3DP)," *Sci. Rep.*, vol. 9, no. 1, Dec. 2019, doi: 10.1038/S41598-019-50583-5.

[20] S. Zhu, M. A. Stieger, A. J. van der Goot, and M. A. I. Schutyser, "Extrusion-based 3D printing of food pastes: Correlating rheological properties with printing behaviour," *Innov. Food Sci. Emerg. Technol.*, vol. 58, no. July, p. 102214, 2019, doi: 10.1016/j.ifset.2019.102214.

[21] A. Perrot, • D Rangeard, and • A Pierre, "Structural built-up of cement-based materials used for 3D-printing extrusion techniques," *Mater. Struct.*, doi: 10.1617/s11527-015-0571-0.

[22] J. P. Kruth, M. C. Leu, and T. Nakagawa, "Progress in additive manufacturing and rapid prototyping," *CIRP Ann. - Manuf. Technol.*, vol. 47, no. 2, pp. 525–540, Jan. 1998, doi: 10.1016/S0007-8506(07)63240-5.

[23] T. J. Wallin, J. Pikul, and R. F. Shepherd, "3D printing of soft robotic systems," *Nat. Rev. Mater.*, vol. 3, no. 6, pp. 84–100, 2018, doi: 10.1038/s41578-018-0002-2.

[24] S. K. Romberg *et al.*, "Linking thermoset ink rheology to the stability of 3D-printed structures," *Addit. Manuf.*, vol. 37, no. September 2020, p. 101621, 2021, doi: 10.1016/j.addma.2020.101621.

[25] H. Zhao, Y. Li, A. Elsamadisi, and R. Shepherd, "Scalable manufacturing of high force wearable soft actuators," *Extrem. Mech. Lett.*, vol. 3, pp. 89–104, 2015, doi: 10.1016/j.eml.2015.02.006.

[26] E. Luis *et al.*, "Silicone 3D Printing: Process Optimization, Product Biocompatibility, and Reliability of Silicone Meniscus Implants," *3D Print. Addit. Manuf.*, vol. 6, no. 6, pp. 319–332, 2019, doi: 10.1089/3dp.2018.0226.

[27] J. Plott and A. Shih, "The extrusion-based additive manufacturing of moisture-cured silicone elastomer with minimal void for pneumatic actuators," *Addit. Manuf.*, vol. 17, pp. 1–14, 2017, doi: 10.1016/j.addma.2017.06.009.

[28] F. B. Coulter, B. S. Coulter, E. Papastavrou, and A. Ianakiev, “Production Techniques for 3D Printed Inflatable Elastomer Structures: Part II-Four-Axis Direct Ink Writing on Irregular Double-Curved and Inflatable Surfaces,” *3D Print. Addit. Manuf.*, vol. 5, no. 1, pp. 17–27, 2018, doi: 10.1089/3dp.2017.0069.

[29] M. Muthusamy, S. Safaee, and R. Chen, “Additive Manufacturing of Overhang Structures Using Moisture-Cured Silicone with Support Material,” *J. Manuf. Mater. Process.*, vol. 2, no. 2, p. 24, 2018, doi: 10.3390/jmmp2020024.

[30] T. P. Sathishkumar, S. Satheeshkumar, and J. Naveen, “Glass fiber-reinforced polymer composites - A review,” *J. Reinf. Plast. Compos.*, vol. 33, no. 13, pp. 1258–1275, 2014, doi: 10.1177/0731684414530790.

[31] A. R. Payne and R. E. Whittaker, “Reinforcement of rubber with carbon black,” *Composites*, vol. 1, no. 4, pp. 203–214, 1970, doi: 10.1016/0010-4361(70)90005-4.

[32] A. F. O., A. P. O., and O. O. O., “Mechanical Properties of a Polyester Fibre Glass Composite,” *Int. J. Compos. Mater.*, vol. 2, no. 6, pp. 147–151, 2013, doi: 10.5923/j.cmaterials.20120206.06.

[33] M. E. Kazemi, M. A. Kouchakzadeh, and M. Shakouri, “Stability analysis of generally laminated conical shells with variable thickness under axial compression,” *Mech. Adv. Mater. Struct.*, vol. 27, no. 16, pp. 1373–1386, 2020, doi: 10.1080/15376494.2018.1511016.

[34] M. Schaffner, J. A. Faber, L. Pianegonda, P. A. Rühs, F. Coulter, and A. R. Studart, “3D printing of robotic soft actuators with programmable bioinspired architectures,” doi: 10.1038/s41467-018-03216-w.

[35] T.-S. Wei *et al.*, “CommuniCation 3D Printing of Customized Li-Ion Batteries with Thick Electrodes,” *Adv. Mater*, vol. 30, p. 1703027, 2018, doi: 10.1002/adma.201703027.

[36] J. O. Hardin, T. J. Ober, A. D. Valentine, and J. A. Lewis, “Microfluidic printheads for multimaterial 3D printing of viscoelastic inks,” *Adv. Mater.*, vol. 27, no. 21, pp. 3279–3284, 2015, doi: 10.1002/adma.201500222.

[37] E. B. Duoss *et al.*, “Three-dimensional printing of elastomeric, cellular architectures with negative stiffness,” *Adv. Funct. Mater.*, vol. 24, no. 31, pp. 4905–4913, Aug. 2014, doi: 10.1002/adfm.201400451.

[38] “Nittany Lion by edsped - Thingiverse,” Oct. 25, 2018. https://www.thingiverse.com/thing:3176601 (accessed May 28, 2021).

[39] Z. Yang, H. Peng, W. Wang, and T. Liu, “Crystallization behavior of poly(ε-caprolactone)/layered double hydroxide nanocomposites,” *J. Appl. Polym. Sci.*, vol. 116, no. 5, pp. 2658–2667, 2010, doi: 10.1002/app.

[40] D. R. Paul and J. E. Mark, “Fillers for polysiloxane (‘silicone’) elastomers,” *Prog. Polym. Sci.*, vol. 35, no. 7, pp. 893–901, 2010, doi: 10.1016/j.progpolymsci.2010.03.004.

[41] P. K. Vallittu, “High-aspect ratio fillers: Fiber-reinforced composites and their anisotropic properties,” *Dent. Mater.*, vol. 31, no. 1, pp. 1–7, 2015, doi: 10.1016/j.dental.2014.07.009.

[42] L. Karásek and M. Sumita, “Characterization of dispersion state of filler and polymer-filler interactions in rubber-carbon black composites,” *J. Mater. Sci.*, vol. 31, no. 2, pp. 281–289, 1996, doi: 10.1007/bf01139141.

[43] S. Nikbakt, S. Kamarian, and M. Shakeri, “A review on optimization of composite structures Part I: Laminated composites,” *Compos. Struct.*, vol. 195, no. March, pp. 158–185, 2018, doi: 10.1016/j.compstruct.2018.03.063.

[44] Dow, “Dowsil SE 1700,” 2017. [Online]. Available: https://consumer.dow.com/en-us/pdp.dowsil^{TM} se 1700.01707116z.html?tab=overview&id=01707116z.

[45] Dow, “EVOLV3D ^{TM} LC 3335 Liquid Silicone Rubber,” no. 45, pp. 2–3, 2017.

[46] DuPont, “Liveo ^{TM} Medical Adhesive Type A,” pp. 4–7, 2020.

[47] Dow Corning, “SILASTIC ® BioMedical Grade Liquid Silicone Rubbers,” *Dow Corning*, 2006, [Online]. Available: http://www.dowcorning.com.

[48] DuPont, “Liveo ^{TM} C6-770 LSR,” 2021.

Appendix

Table 3. UTS of Sample Set 1

Material	20% infill	30 % infill
ABS	3.139 MPa	4.332 MPa
Nylon	4.172 MPa	4.101 MPa
PETG	3.806 MPa	4.334 MPa

Table 4. Youngs Modulus of Sample Set 1

Material	20% infill	30 % infill
ABS	2.317 MPa	2.843 MPa
Nylon	2.385 MPa	3.051 MPa
PETG	4.468 MPa	4.451 MPa

Table 5. UTS and Modulus for Sample Set 2

Grid Pattern	UTS (MPa)	Youngs Modulus (MPa)
45°/45° Grid	3.608	2.498
Triangles	1.412	1.509
Triangles (rotated 90°)	2.019	2.222
Octet 0°/90°	3.501	6.749
0°/20°/340° Grid	3.447	27.369
Tri-Hex	3.297	4.296
Tri-Hex (rotated 90°)	3.445	4.940

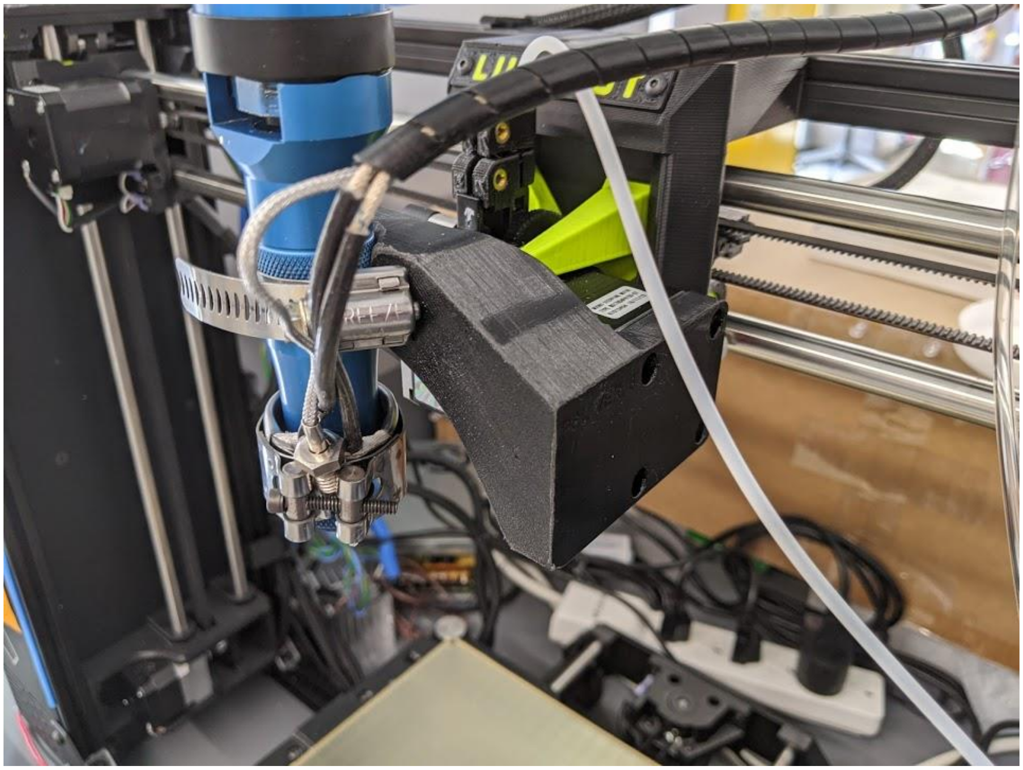

Figure 15 Silicone extruder (blue) in printed silicone arm (black)

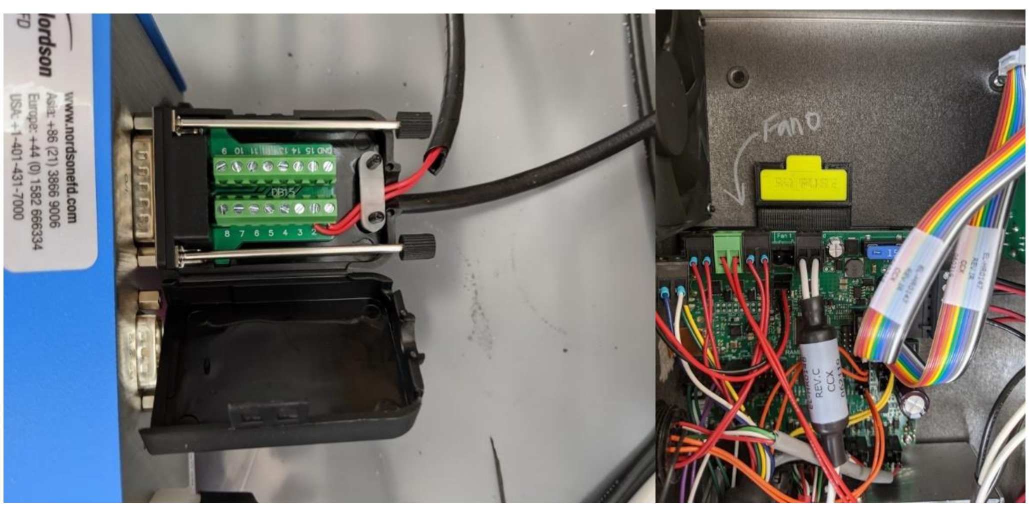

Figure 16 (Left) I/O connection for Nordson Ultimus (right) I/O connection to Fan 0 pins in the Lulzbot

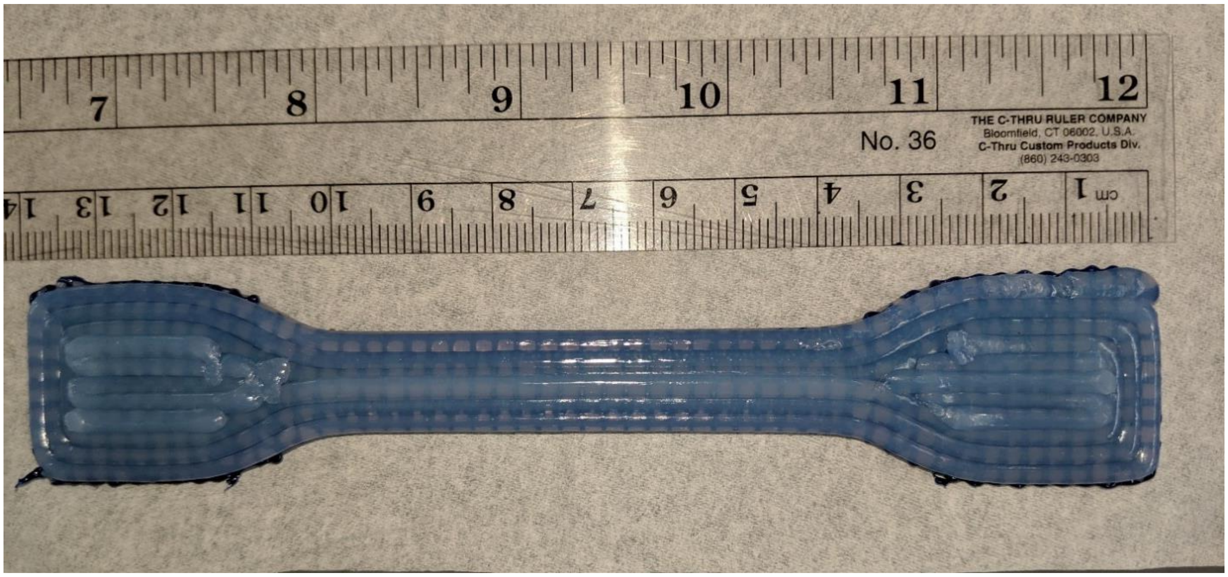

Figure 17. 30% PETG Tensile bar

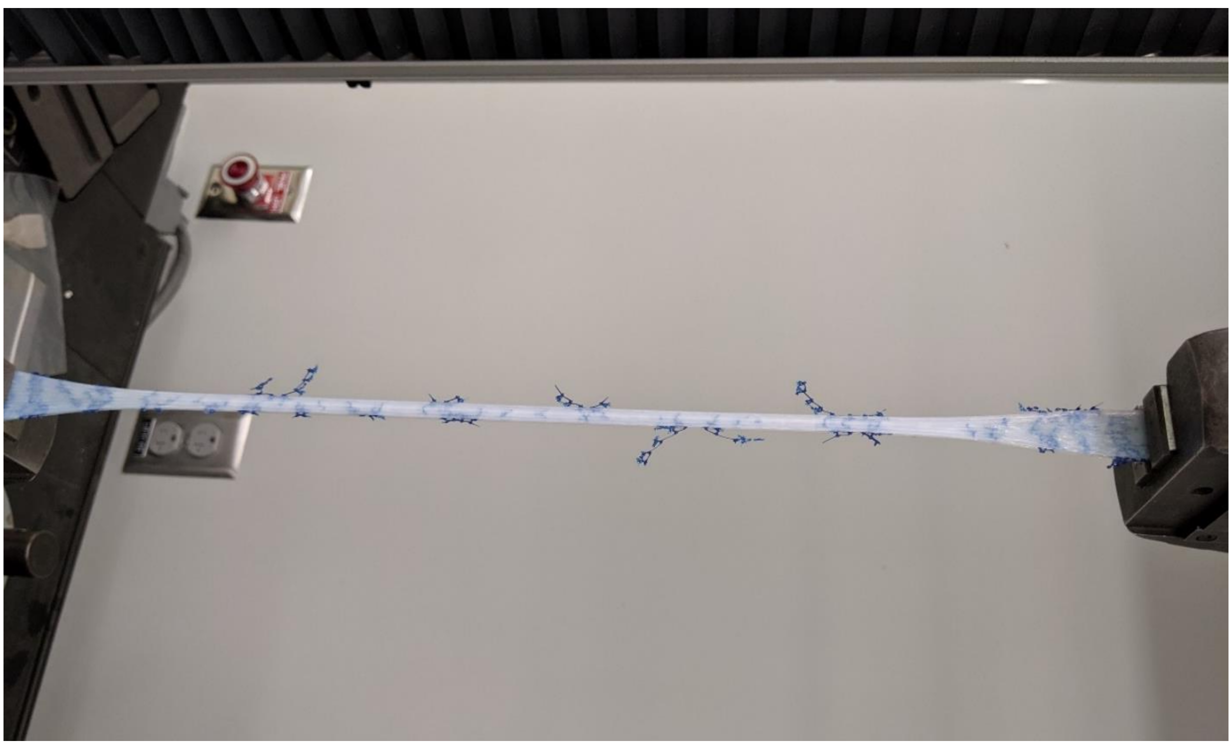

Figure 18. 30% PETG Tensile bar mid testing. The failure of the mesh is visible.

Figure 19. 3DBenchy printed with Liveo C6-770 silicone (high viscosity near zero shear). US nickel for scale.

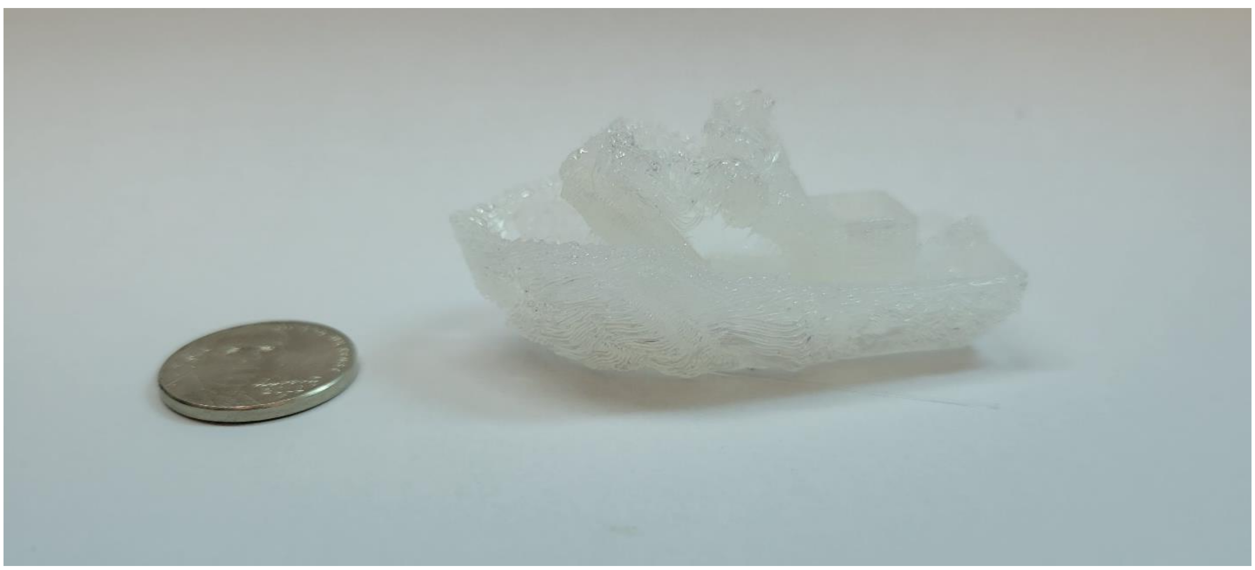

Figure 20. 3DBenchy printed with SE-1700 silicone (low viscosity near zero shear). US nickel for scale.